IEEE Access
Multidisciplinary | Rapid Review | Open Access Journal

IEEE ENGINEERING IN MEDICINE AND BIOLOGY SOCIETY SECTION

Received June 12, 2021, accepted July 7, 2021, date of publication August 16, 2021, date of current version August 20, 2021.

Digital Object Identifier 10.1109/ACCESS.2021.3104985

Blind and Robust Watermarking Scheme in Hybrid Domain for Copyright Protection of Medical Images

ALI ALZAHRANI AND NISAR AHMED MEMON

Department of Computer Engineering, College of Computer Sciences and Information Technology (CCSIT), King Faisal University, Al-Ahsa 31982, Saudi Arabia

Corresponding authors: Ali Alzahrani (aalzahrani@kfu.edu.sa) and Nisar Ahmed Memon (nmemon@kfu.edu.sa)

This work was supported by the Deanship of Scientific Research at King Faisal University under Grant 216014.

This work involved human subjects or animals in its research. The authors confirm that all human/animal subject research procedures and protocols are exempt from review board approval.

ABSTRACT This work presents a robust watermarking technique in hybrid domain for the copyright claim of medical images. The scheme is a fusion of three popular transforms: Discrete Wavelet Transform (DWT), Discrete Cosine Transform (DCT) and Singular Value Decomposition (SVD). The input image is first separated into region of interest (ROI) and region of non-interest (RONI). The DWT is applied on RONI to get low and high frequency bands. The low frequency band is then segmented into 4×4 blocks. The Human Visual System (HVS) is applied to select the potential blocks for implanting watermark content. Each 4×4 selected block is further subdivided into four 2×2 carrier matrices. The SVD is applied to each carrier matrix. Finally, the hidden information is implanted by altering the largest diagonal singular values of four 2×2 matrices. The technique is blind, so host image is not needed for the extraction of hidden information. The proposed scheme achieves higher values of imperceptibility as well as robustness. Experimental results reveal that the proposed technique outperforms the techniques currently reported in the literature by achieving higher values of imperceptibility in the form of PSNR with value of 44.0567 decibels (dB) and SSIM value of 0.9800. At the same time it achieves excellent values of robustness with maximum NCC value of 1.000 and minimum BER with value of 0.000.

INDEX TERMS Medical image watermarking, copyright protection, singular value decomposition, medical images, ROI and RONI.

I. INTRODUCTION

Nowadays, medical practitioners usually exchange medical images of patients produced from different modalities in digital form over public networks like Internet. These images are exchanged for clinical interpretation with other radiologists and physicians working in the same field [1]. Internet is information highway where everybody can share information with each other freely. Due to the development of current computer technologies, people can store, duplicate and distribute information over the Internet [2]. This has resulted in increase of both intentional and unintentional attacks on copyrighted digitized data. Recent studies [3], [4] reveal that unauthorized use of medical data is increasing on daily basis. This mishandling of medical information can raise copyright and privacy issues when it is exchanged from one geographical region to another over the Internet [5].

Various methods of hiding information such as digital image watermarking, cryptography, steganography are in common practice to resolve the issues of copyright and secrecy of medical images and patients' diagnostic as well as personal information. Among these techniques, digital image watermarking [6]–[10] has attracted the attention of researchers because it has a lot of characteristics that can help to resolve the issues of copyright protection and security of medical information.

There are two domains in which digital image watermarking is carried out: (i) spatial domain [11]–[13], where information is hidden in the host image by altering the pixel gray levels (ii) Frequency domain [14]–[16], where the input

The associate editor coordinating the review of this manuscript and approving it for publication was Henry Hess.

signal is converted into frequency domain, after which the hidden information is embedded by altering the frequency coefficients.

Watermarking is also classified in relation to the process of extracting watermark. A technique can be called non-blind if the host and the watermark images are required for extracting the watermark. If the secret key and the watermarked image are used for extracting the watermark it is known as semi-blind watermarking. Now, if only the secret key is needed for extracting the watermark then it is called bind watermarking scheme [8], [17].

Two other categories of watermarking are (i) Robust watermarking and (ii) Fragile watermarking. These categories depend on the application or purpose of the watermarking. The main purpose of robust watermarking [12], [18]–[21] is the robustness of hidden information, that is, how embedded information can survive or resist attacks launched by an invader during transmission of data. Thus, robust watermarking is popular for copyright protection of digital data. On the other hand, fragile watermarking [22]–[25] is used to find the area tampered with by an invader, that is, the area of the watermarked image tampered with during transmission. Thus, fragile watermarking is used to check the integrity of the content of digital data.

As frequency domain watermarking has more advantages than spatial domain watermarking, researchers usually use frequency domain watermarking techniques. DCT, DWT and SVD are more popular transforms which are used in frequency domain watermarking techniques. These transforms can be used combined and is called hybrid domain watermarking. The hybrid domain methods can increase the performance of the watermarking technique.

Imperceptibility and robustness are two important criteria which are taken into consideration when new robust watermarking technique is developed. SVD has attractive properties. For example, singular values of host image have high resistance even if small amount of noise is introduced [26], [27]. Due to this characteristic of SVD, a number of researchers have introduced SVD-based watermarking [28]–[30].

A novel robust and blind watermarking scheme is presented here in hybrid domain. The scheme is a fusion of 3 transforms: DWT, DCT and SVD. The technique is proposed for the following reasons:

(1) To get high imperceptibility of watermarked image.
(2) To provide copyright protection of medical images.
(3) To maintain the security of patients' information.

II. RELATED WORK

Seenivasagam and Velumani [31], in their study, reported a secure and blind watermarking technique. They used Quick Response (QR) code as watermark, which was scrambled through Arnold transform before implanting. The technique presented zero watermarking which exploited the contourlet transform (CLT) in SVD domain without any embedding. In this technique, the host image was not degraded because zero watermarking was utilized to implant the hidden information logically in the host signal. To check the imperceptibility of the watermarked image, the structured similarity index measure (SSIM) metric was used; whereas Bit error rate (BER) and Normalized Correlation (NC) metrics were used to verify the robustness of the proposed technique. 512×512 size image was used as cover image, whereas watermark image of 77×77 size was used in simulations. The following medical images, CT, Mammogram, MRA, PET, Ultrasound, Nuclear and XRAY were used for the experiments.

Singh *et al.* [32] used a non-blind technique which was developed in hybrid domain, consisting of three transforms DWT, DCT and SVD. Images and text characters were used as watermark and embedded in medical images. In order to reduce the encryption-decryption, computational time low encryption algorithm was used for encrypting the text watermark. The image with 512×512 size was used as cover image while that with 256×256 size was used as watermark. Also, 50 characters of text watermark were implanted in the cover image. The scheme reported PSNR values of 35.84 dB.

Zhou *et al.* [33] reported a robust method which is based on DWT, all phase discrete cosine biorthogonal transform (APDCBT) and SVD. To enhance the visibility of the watermarked image, direct current (DC) coefficients after block-based APDCBT in high frequency sub-bands were altered with watermark. The watermarked image had higher image quality as analyzed with other SVD-based watermarking schemes. The scheme had high robustness against many legitimate and illegitimate attacks.

Ahmadi *et al.* [34] presented a blind watermarking method in which DWT, SVD, HVS and Particle Swarm Optimization (PSO) algorithm were utilized. First, the DWT was applied up to 1^{st} level, and then LL1 was utilized to implant the hidden information. The HVS was exploited in the proposed scheme to achieve higher imperceptibility. SVD was then applied on the resultant blocks which passed the test of HVS. The two watermark bits were embedded in U and V components obtained after applying SVD. Experimental results demonstrate the stability of the method.

Soliman *et al.* [35] presented a hybrid method which is a fusion of PSO, adaptive quantization index modulation (AQM), SVD and DWT. The scheme provides better security, secrecy and integrity of medical images. The PSO algorithm is used successfully to improve the robustness of the scheme and watermarked image quality. The scheme reports PSNR value of 52.28 dB. The medical images (XRAY of chest, skull, liver and kidney) of size 512×512 were used in the experiments as cover images; whereas, a binary image of size 32×32 was used as watermark. One limitation of the scheme is that the computational complexity of the algorithm is high, though it can be reduced.

Zear *et al.* [36] studied a watermarking method exploiting DWT, DCT and SVD. The authors used three watermarks, namely lump image as image watermark, doctors' ID

and patients' diagnostic information. The Back Propagation Neural Network (BPNN) was exploited for improving the robustness of the technique. The Arnold Transform was used for scrambling the image watermark before implanting it into the cover image. The lossless arithmetic encoding scheme along with Hamming error correcting codes was used to compress patients' diagnostic information before implanting it in the cover image. The cover images of different modalities along with text watermarks of different sizes were used in the experiments. The simulations demonstrate that the method withstands different legitimate and illegitimate attacks.

Ernawan *et al.* [37] used a blind watermarking technique that embedded multiple watermarks in cover image based on HVS characteristics. In the technique some threshold value was used to find the watermark values by altering the first column of orthogonal U matrix obtained after applying SVD. The optimal threshold was obtained by adjusting balance among Normalized Cross Correlation (NC) and the imperceptibility of watermarked image. The scheme reports the results which show that multiple watermarks provide remarkable robustness against different attacks.

Alias *et al.* [38] reported another multiple watermarking technique in which optimal threshold technique was used. The scheme utilized the DWT in conjunction with SVD transform. The scheme embedded multiple watermarks which serve for more than one copyright claims. To embed multiple watermarks, HVS characteristics were considered. The color cover images were used in the experiments. Multiple watermarks were implanted into red and blue color components of the cover image. The scheme utilized the U orthogonal matrix to embed and extract the watermark. To increase the security of watermarks, the Arnold Transform was used to scramble and implant them in the cover image. The optimal thresholds were calculated by adjusting tradeoff between the imperceptibility and NC values. The scheme reports better results against a number of attacks.

Thakkar *et al.* [39] reported another scheme using DWT and SVD transforms. The host image was separated into ROI and RONI first. Later DWT was applied on ROI to get low and high frequency components. After then, SVD was applied on LL blocks to obtain singular matrices. These matrices were altered for implanting the hidden information by selecting an appropriate threshold in order to control the imperceptibility and robustness of the watermarked image. Two different watermarks, logo and text information are used for copyright protection and identification purpose, respectively. It is a blind technique, that is, no original image is needed for extracting the hidden information. Different medical images are used, for example XRAY, CT and Mammography. The scheme reports PSNR values above 43 dB for watermarked images.

Another watermarking scheme for medical images was presented by Liu *et al.* [40]. Usually, in medical image watermarking, the host image is separated in ROI and RONI. The information related to ROI is implanted in RONI for authentication and recovery of watermark information. This is because this process may create biases on diagnosis and can introduce security risks by segmenting image spatially for watermark embedding. This important issue was addressed in the scheme proposed in [40]. The scheme exploits recursive dither modulation (RDM) to control biases on diagnosis. The scheme uses RDM plus Slantlet Transform (SLT) and SVD for protecting image authenticity. The scheme reports better imperceptibility and robustness of watermarked image.

Thabit and Khoo [41] reported another technique addressing the issues of robustness of authentication of watermarking scheme against legitimate and illegitimate attacks. The cover image was separated into ROI and RONI, and then SLT was exploited to implant watermark information in both regions. For extracting the hidden information at the receiving end Integer Wavelet Coefficients were utilized. The simulations results proved that the proposed scheme can withstand legitimate attacks like JPEG compression, additive Gaussian Noise (AGN) and salt and pepper Noise.

There are four important concerns for digital watermarking, namely, imperceptibility, robustness, capacity and security. Researchers have been trying numerous methods to improve these four aspects. Because original host images are not always accessible at the receiving side, the watermark detection is often proceeded without referring to the primordial data. Under such a blind condition, many watermarking methods suffer various degrees of deficiencies in robustness, transparency, and payload capacity. Therefore, an effective blind and robust watermarking scheme is presented which addresses these four issues. Imperceptibility and robustness has been increased by combining three transforms, namely DWT, DCT and SVD. Capacity has been increased by taking small carrier matrices size 2×2, whereas security is achieved by encrypting watermarks by encrypting them through different algorithms.

III. TOOLS AND TECHNIQUES

The tools and techniques given below are used for the development of the watermarking scheme presented in this paper.

A. SINGULAR VALUE DECOMPOSITION (SVD)

Recently, SVD has attracted researchers. SVD is a powerful tool used in linear algebra. It is used in a number of areas, for example image compression, watermarking and other signal processing applications. SVD is defined as given in Eq. 1

$$A = U * S * V^T \tag{1}$$

where A is n × n matrix, U and V are two orthogonal matrices and S is a diagonal matrix consisting of the singular values of A. The singular values satisfy the following property,

$$s(1, 1) > s(2, 2) > s(3, 3) > \ldots\ldots\ldots > s(n,n) > 0 \tag{2}$$

and superscript T represents the matrix transposition. SVD is used in a number of watermarking techniques [38], [39]. It has the following attractive properties:

(i) Large portion of signal energy can be represented by few singular values, (ii) Both square and rectangular sized

TABLE 1. Original and changed singular values after attacks.

Attack	S1 (1)	% of change (2)	S2 (3)	% of change (4)	S3 (5)	% of change (6)	S4 (7)	% of change (8)
Lena Image (Original values)	253.8552	---	41.5537	---	32.061	---	25.3938	---
JPEG Compression (QF=20)	253.8381	0.0067	41.6087	0.1323	32.0201	0.1275	25.3367	0.2248
JPEG 2000 (CR=3)	253.9831	0.0503	41.556	0.0055	32.0444	0.0517	25.3903	0.0137
Rotation 2 degree (clockwise)	253.2211	0.2497	42.112	1.3435	32.4297	1.1499	25.3752	0.0732
Scaling (512→ 256→512)	253.8764	0.0083	41.5398	0.0334	32.0357	0.0789	25.3649	0.1138
Scaling (512→ 1024→512)	253.8704	0.0059	41.5512	0.0060	32.0576	0.0106	25.3878	0.0236
Average Filter [3 × 3]	253.3309	0.2065	41.3723	0.4365	32.886	2.5732	25.2857	0.4256
Gaussian Noise (m=0, var=0.01)	253.8795	0.0095	41.6287	0.1804	32.1481	0.2716	25.7225	1.2944
Salt & Pepper (m=0, var=0.01)	253.7737	0.0321	41.1202	1.0432	32.7507	2.1512	25.1775	0.8517
Wiener Filter [3 × 3]	253.8368	0.0072	41.5833	0.0712	32.1699	0.3396	25.423	0.1149
Median Filter [3 × 3]	253.6182	0.0933	41.676	0.2943	32.146	0.2651	25.4706	0.3024
Histogram Equalization	253.8552	0	41.5537	0	32.061	0	25.3938	0
Cropping [25 25 512 512]	253.5199	0.1320	41.395	0.3819	32.3686	0.9594	25.9469	2.1780
Average		0.0711		0.3976		0.8018		0.3776

images can be utilized by SVD, (iii) Due to its good immunity to noise, singular values are not changed significantly when small perturbation is added to an image intensity values, (iv) Singular values represent the intrinsic algebra of an image.

In order to check the immunity of singular values to noise, an experiment was carried out. The 8-bit gray scale image Lena of size 512 × 512 was used for the experiment. The singular values obtained after applying different attacks were compared with four most significant singular values of Lena image. Table 1 shows the results. Columns 1, 3, 5, 7 of Table 1 show the singular values and columns 2, 4, 6, 8 show the percentage of increase or decrease in these values after attack. The average of columns 2, 4, 6 and 8 shows that the change in singular values is almost less than one percent in each attack. Thus, it can easily be concluded from the values shown in Table 1 that singular values are more resistant and can withstand small perturbation. Due to this resistance against noise, SVD has attracted the attention of researchers and has become a popular domain in watermarking.

Based on the reasons specified above, the singular values matrix was chosen as a carrier of hidden information, and the highest diagonal value was selected for embedding the watermark information.

B. SELECTION OF OPTIMUM THRESHOLD FOR EMBEDDING

To find a better balance between the imperceptibility and robustness of the proposed scheme, the optimum threshold was selected after carrying out a number of experiments. Generally, in literature, the NC and SSIM metrics are used to check the robustness and imperceptibility of watermarking technique. The values of these two metrics lie in the range of [0 1]. Therefore, for the proposed scheme, the optimum threshold was selected by setting the better tradeoff between NC and SSIM. Four attacks: JPEG Compression (with quality factor = 30), Gaussian Noise with density (D = 0.002), Salt and Pepper with noise density (D = 0.005) and low pass filter attack were applied on the test images (XRAY, CT, Ultrasound and MRI). The average values were calculated by setting threshold values in the range of [10–100] with the step of 10. The results are depicted in the graphs as given in Fig. 1(a-d). It can be observed from Fig 1(a-d) that with increase in the value of T, the value of SSIM decreases while the value of NC increases. Thus, the values where SSIM and NC intersect are selected as the optimal threshold. Values 54, 50, 50, and 50 are selected as the optimal threshold for CT, XRAY, Ultrasound and MRI medical images, respectively.

C. SEGMENTATION OF MEDICAL IMAGE

The geometrical shapes such as square and rectangle were used to draw a boundary for ROI on each medical image. This boundary was used to separate the cover medical image into ROI and RONI before implanting the hidden information. As shown in Fig. 3, the proposed scheme avoided embedding the watermark content in the ROI. A binary mask was created for each medical image based on this boundary. Black pixels in the binary mask represent RONI region, whereas white pixels represent the ROI. The blocks of RONI which overlap with ROI are avoided during the embedding of the watermark information to ensure that the watermark is not destroyed during the segmentation. The spatial coordinates of geometrical shapes square or rectangle are stored as side information. The same were extracted at the decoder side and were used to draw the same geometrical shape for marking the ROI on the watermarked image. Different ROIs selected on input images are shown in Fig 5.

D. SELECTING THE SMALL BLOCK SIZE FOR EMBEDDING WATER MARK INFORMATION

It was indicated by Dowling *et al.* [42] in their comparison between the DWT and DCT block-based watermarking that the DCT approach is more effective at smaller block sizes while the DWT approach is probably superior if the watermarking is applied to the entire image. In [43], Al-Haj proposed using a combination of DWT and DCT to

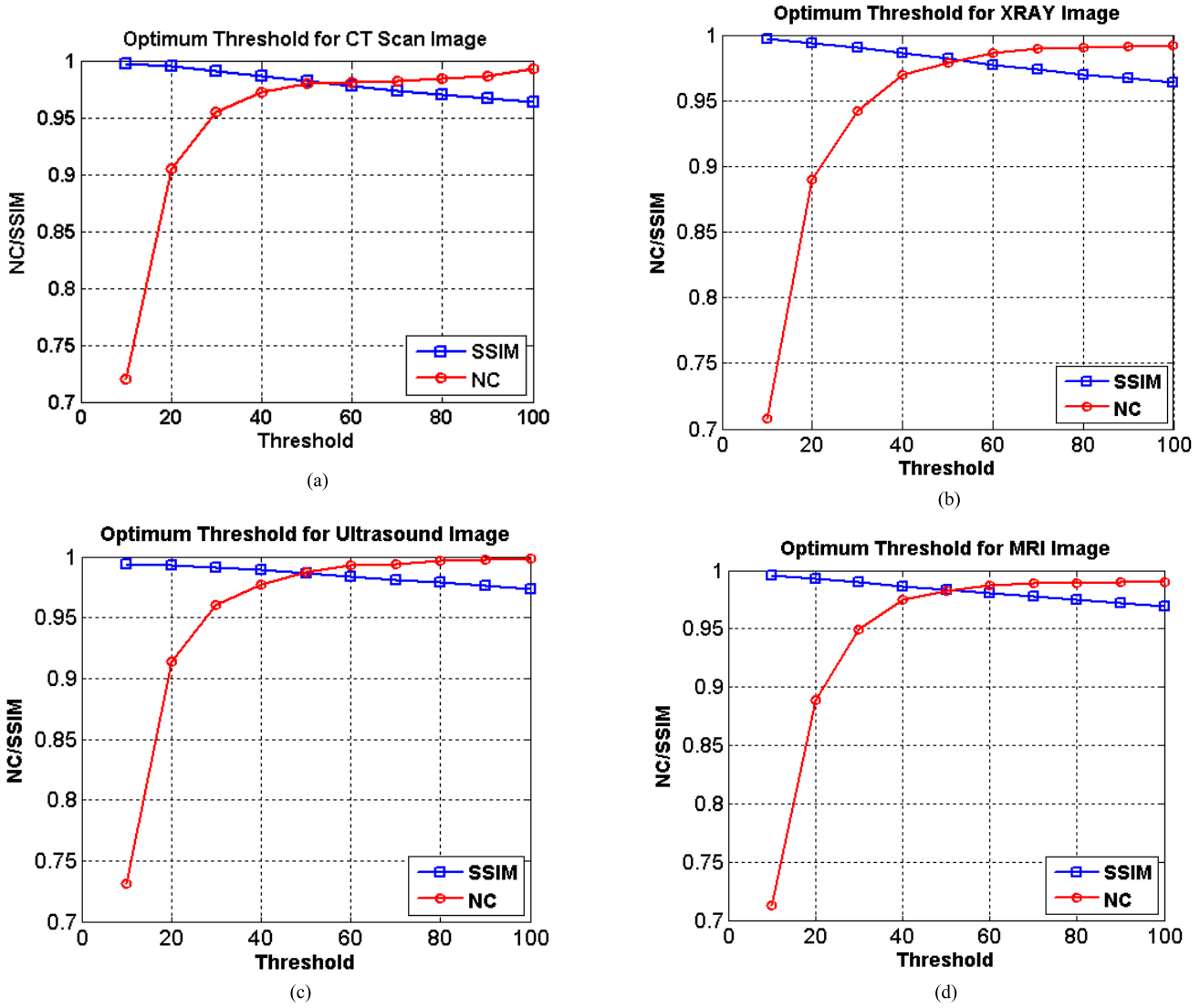

FIGURE 1. Optimum thresholds selected for different medical images.

implement blind image watermarking. After applying DWT to decompose the host image into multi-resolution sub-bands, he divided the selected sub-bands into blocks of size 4×4. Each block was then converted to DCT representation. Binary embedding was carried out by adding uncorrelated pseudo-random sequences to the middle-frequency DCT coefficients. Several other DWT-DCT based watermarking algorithms were developed later based on Al-Haj's framework.

In principle, a block-based scheme deals with every block separately, thus providing several advantages when small block size is selected.. For example, we can exploit the distinct features (such as local luminance and texture) of each individual image block to improve the robustness of the embedded watermark and/or enhance the visual quality of the watermarked image [44]. We can use a different secret key in each block to reinforce the security of the watermark. The amount of information bits may also vary from one block to another. Moreover, the block-based schemes are very suitable for applications dedicated to the regions of interest (ROI) and region of non-interest (RONI). The proposed scheme follow the same mechanism defined in [43] is followed.

E. HUMAN VISUAL SYSTEM (HVS)

The characteristics of HVS are being exploited to identify the most suitable region to embed the watermark information in the host image. HVS characteristics are utilized to determine the suitable embedding locations during implanting of watermark [37], [38]. The entropy was used to measure the spatial correlation of neighbor pixels. The entropy of an N-state is defined in Eq. 3.

$$E = -\sum_{i=1}^{N} P_i \log_2(P_i) \tag{3}$$

Image edge is an important information of image characteristics. Edge entropy of an image block is considered for embedding regions. Edge entropy is defined in Eq. 4,

$$E_{edge} = -\sum_{i=1}^{N} P_i \exp^{1-p_i} \tag{4}$$

where P_i denotes the occurrence probability of i-th pixel with $0 \leq P_i \leq 1$ and $1-P_i$ represents the uncertainty or ignorance of the pixel value. The values obtained from combination between entropy and edge entropy are sorted in ascending order and the lowest value are chosen as embedding regions. For combination between entropy and edge entropy is defined in Eq. 5.

$$HVS_E = \sum_{i=1}^{N} P_i \log_2(P_i) - P_i \exp^{1-p_i} \tag{5}$$

IV. PROPOSED SCHEME

Medical image watermarking is challenging compared to natural image watermarking due to the following reasons [39]: (1) The watermarked medical image should be highly imperceptible as it is required by medical practitioner for diagnosis (2) Since the ROI of medical image is crucial to physicians for diagnosis purpose, its integrity should not be compromised and (3) Simple codes required for authentication are not sufficient, but electronic patients' record (EPR) consisting of details such as name, age, sex, name of physicians need to be implanted in the medical image [45].

A robust and blind hybrid watermarking scheme is presented in this paper, which is a combination of three different transforms: DWT, DCT and SVD. The fusion of these transforms makes the proposed technique highly imperceptible and robust against various unintentional and intentional attacks. Thus, it fulfills the requirements of watermarking algorithm generally required for medical images. First, the host image is separated into ROI and RONI. Then DWT is applied on RONI to get low and high frequency bands. The low frequency band is further segmented into blocks of size 4×4. The HVS system is applied on these blocks, and blocks passing the test of HVS are selected for embedding; also, their corresponding x and y coordinates are recorded. DCT was performed on each block and DCT coefficient matrix C was produced. C was further subdivided into 2×2 block matrices referred to as information carrier matrices B1, B2, B3 and B4. Finally, SVD was applied on each carrier matrix. The hidden information was then implanted into S singular values. Recently, Cheng et. al. [46] reported a DCT-SVD based scheme in Contourlet Transform (CLT). After applying CLT on the cover image, the LL frequency band was segmented into blocks of size 8×8 and DCT was applied on them to get coefficient matrix D. The D was scanned in zigzag order to generate row vector. Then from this row vector some coefficients were selected to create two carrier matrices M1 and M2 of 2×2 size.

To implant the hidden information SVD was applied on these two matrices and singular values of this pair of matrices were modified to achieve blind extraction for natural images. Using this property of the pair of carrier matrices created from DCT transformed block, the copyright information and EPR were implanted in the RONI region of the medical image. As far as watermarking of medical images is concerned, it was observed by Cheng [46] that, when ROI is avoided from embedding the watermark information based on the requirements of medical image watermarking, more blocks would be needed to embed watermark information. So, we modified the technique [46] and made one change. Medical images usually contain black background which results in the creation of zero blocks when RONI is divided in non-overlapping blocks of small sizes of 2×2, 4×4 and 8×8. Also, these zero blocks do not allow to embed the watermark information when they are decomposed in SVD domain. Due to these reasons, in the proposed technique, we avoided implanting the watermark information in zero blocks, and thus increased the embedding capacity to embed two bits of watermark information in single block instead of one bit. By this way, the proposed technique not only increases the embedding capacity of algorithm but also withstands different types of attacks.

Thus, in the proposed technique, first DWT was applied on medical image to obtain low and high frequency sub-bands. Later, low frequency band (LL) was segmented in ROI and RONI regions. The RONI part was segmented into blocks of size 4×4. DCT was applied to obtain DCT coefficient matrix C. After then, the scheme embedded two bits per block by selecting the four carrier matrices of each DCT coefficient matrix C for implanting and getting back the watermark information in the S matrix after applying SVD on these carrier matrices. Based on the watermark content, the pair of diagonal elements S1(1,1) and S2(1,1) was used for embedding watermark1 information. Similarly, the pair of diagonal elements S3(1,1) and S4(1,1) was used for embedding watermark2 information. The complete detail of the embedding and extraction of watermark information is given in the following sections.

Two watermarks were implanted in the host image for copyright protection and identity of medical image which are referred as to watermark1 and watermark2. The watermark1 serves as ownership watermark. The sample hospital logo of size 32×32 is taken as watermark1 and is used for copyright protection as shown in Fig. 2. The watermark2 is the text watermark which is referred to as EPR and gives the details of the patients' name, ID, registration number, age, sex and the details of the doctor who created or diagnosed the medical image. In order to increase further the security of watermarks, logo is encrypted by applying Arnold Transform using key and EPR is encrypted by XOR with some pseudo

FIGURE 2. The hospital logo.

randomly generated vector. A total 2048 bits or 2K bits ($32 \times 32 = 1024$ bits of logo) + (128 characters of EPR = $128 \times 8 = 1024$ bits) = 2048 bits are embedded in input image.

A. THE EMBEDDING PHASE

In the proposed scheme, the most significant diagonal elements S1(1,1), S2(1,1), S3(1,1) and S4(1,1) of singular values of S1, S2, S3 and S4 obtained from certain blocks of LL band were utilized. These diagonal elements were altered based on the watermark bit of both watermark1 and watermark2. The method used for such embedding of the watermarks is given below:

Algorithm 1 Adjust the values of S1(1,1) and S2(1,1) for embedding the watermark bit 1 or 0 of watermark1 (logo)

Output: S1(1,1) – S2(1,1) > 0

Process

1 $m_1 = (|\ S1(1,1) + S2(1,1)\ |)/2$
2 **If** $\mathbf{w_1(i) = 1}$
3 S1'(1,1) = sign(S1(1,1)) ∗ m_1 + T/2;
4 S2'(1,1) = sign(S2(1,1)) ∗ m_1 − T/2;
5 **Else**
6 S1'(1,1) = sign(S1(1,1)) ∗ m_1 − T/2;
7 S2'(1,1) = sign(S2(1,1)) ∗ m_1 + T/2;
8 **End**

End of process

Algorithm 2 Adjust the values of S3(1,1) and S4(1,1) for embedding the watermark bit 1 or 0 of watermark2 (EPR)

Output: S3(1,1) – S4(1,1) > 0

Process

1 $m_2 = (|\ S3(1,1) + S4(1,1)\ |)/2$
2 **If** $\mathbf{w_2(i) = 1}$
3 S3'(1,1) = sign(S3(1,1)) ∗ m_2 + T/2;
4 S4'(1,1) = sign(S4(1,1)) ∗ m_2 − T/2;
5 **Else**
6 S3'(1,1) = sign(S1(1,1)) ∗ m_2 − T/2;
7 S4'(1,1) = sign(S2(1,1)) ∗ m_2 + T/2;
8 **End**

End of process

In the above singular values adjustment algorithms, '*T*' represents the threshold value used for inserting the hidden data in the host image. The steps of embedding the two different watermarks into RONI are explained below and block diagram is depicted in Fig. 3.

1. Input the cover medical image and the two watermarks logo and EPR.
2. Encrypt the logo by applying Arnold transform using the key, *k*.
3. First convert each alphanumeric character of EPR into its equivalent binary value and generate the binary vector by collecting these binary values. XOR this binary vector with pseudo vector of same size with the key, *k*.
4. Create the binary sequences of the new versions of both logo and EPR. These coded sequences are to be embedded into medical image.
5. Apply DWT on input image up to 1st level to obtain LL, HL, LH and LL bands.
6. Segment the LL band into ROI and RONI regions and store the coordinates of geometrical shape used for segmentation in separate store.
7. Partition RONI into blocks of size 4×4.
8. Apply HVS on selected blocks to select most suitable blocks for embedding the watermark information.
9. Apply DCT on each selected block to create DCT coefficients matrix C.
10. Divide C further into four sub-blocks of size 2×2 referred to as B1, B2, B3 and B4.
11. Apply SVD to generate U, S, and V matrices for each sub-block.
12. Insert the watermark bit using the optimal threshold, *T* into diagonal elements of S matrix by altering the elements S1(1, 1) and S2(1, 1) according to Algorithm 1 and elements S3(1, 1) and S4(1, 1) according to Algorithm 2.
13. Compute the inverse SVD of each sub-block to get watermarked carrier matrices.
14. Merge four modified carrier matrices and compute inverse DCT to get watermarked LL band block.
15. Repeat steps 8–13 until the last bit of each watermark content is completed.
16. To get watermarked RONI', apply inverse DWT on the watermarked LL' and original HL, LH, HH sub-bands.
17. Combine the watermarked RONI' and original ROI to get the watermarked image.

B. THE EXTRACTION PHASE

1. Read the watermarked image.
2. Apply DWT on the watermarked image to get LL', HL, LH and HH sub-bands.
3. Divide the LL' band into ROI and RONI regions based on coordinates which were used at the time of embedding.
4. Partition RONI into sub-blocks of size 4×4.
5. Find the blocks in which the watermark content was inserted.
6. Apply DCT to obtain DCT coefficients matrix C'.
7. Divide C' further into four sub-blocks of size 2×2 referred to as B1', B2', B3' and B4'.
8. Apply SVD to create three matrices U', S', and V' for each sub-block.
9. In a block, if the difference of S1(1,1) - S2(1,1) is greater than 0, consider extract watermark1 as 1 bit, otherwise consider it as 0 bit.
10. Repeat the step 9 for extracting watermark2 from pair S3(1,1) and S4(1,1).

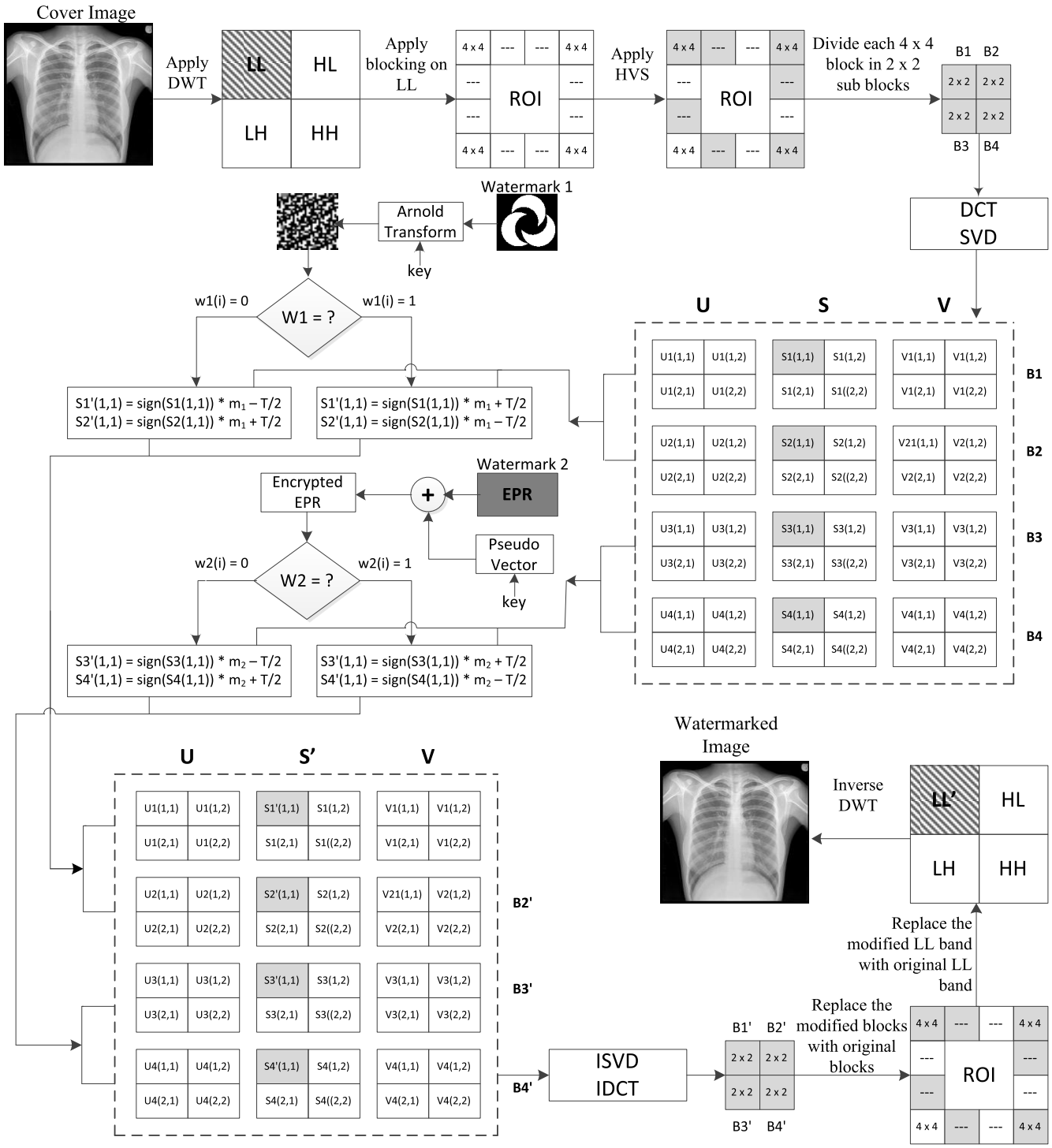

FIGURE 3. The block diagram of embedding algorithm.

11. Reshape the binary sequence of extracted watermark1 to reconstruct the encrypted watermark1 and apply the inverse Arnold Transform to get back the original logo.
12. XOR the extracted watermark2 with pseudo generated binary vector to get the EPR binary sequence.
13. Convert back the binary sequence to alphanumeric characters to get the original patients' information.

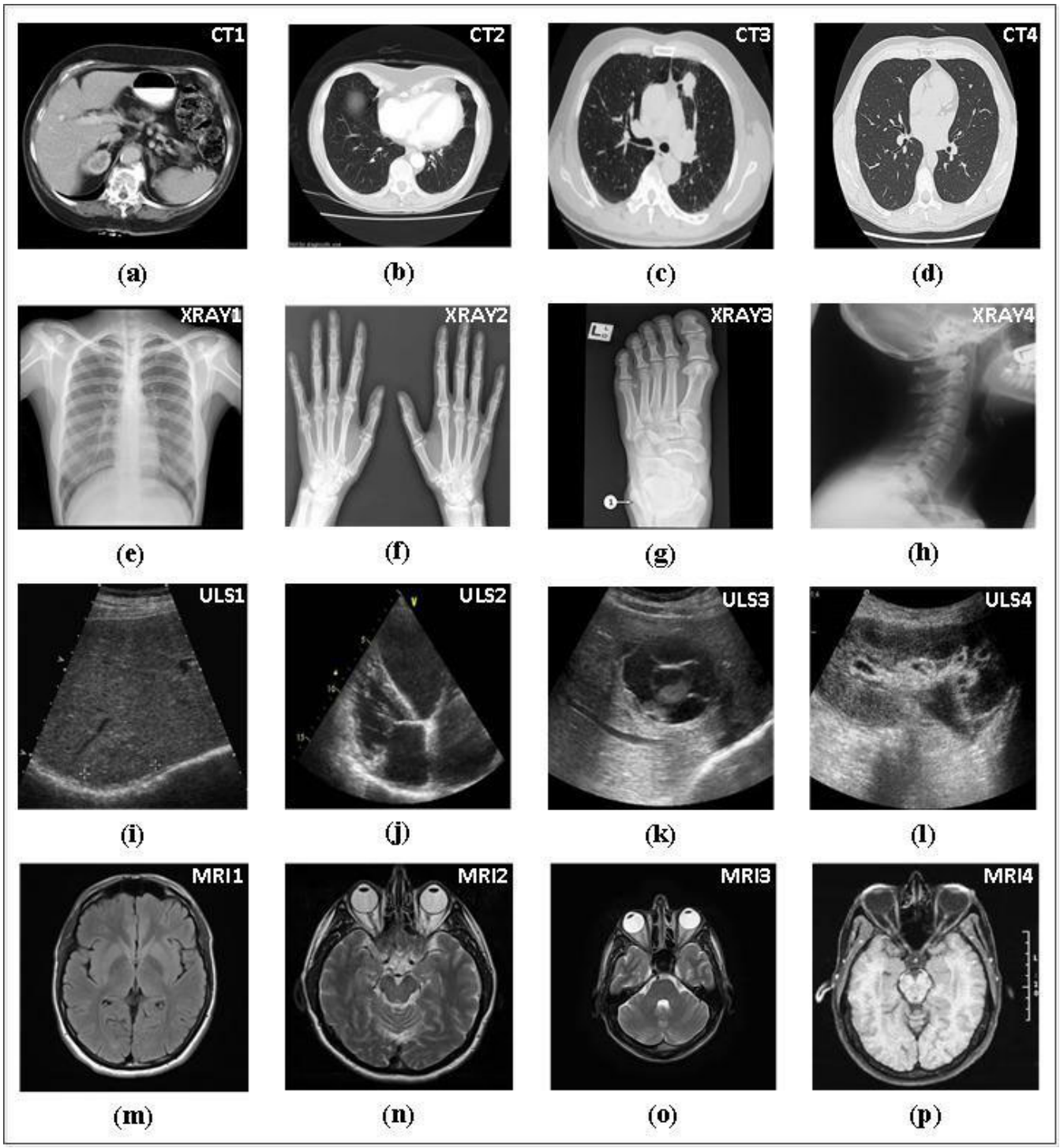

FIGURE 4. Medical images used in simulations.

V. EXPERIMENTAL RESULTS AND DISCUSSIONS

A. EXPERIMENTAL SETUP

The proposed watermarking algorithm is tested on different images such as CT scan, X-ray, Ultrasound and MRI. All medical images used are of size 1024 × 1024 pixels. The test images are depicted in Fig. 4. The MATLAB 2018a software is used for simulations, and Core i5, with 32GB RAM is used as hardware for running the simulations.

B. IMPERCEPTIBILITY ANALYSIS

The imperceptibility analysis of the scheme was conducted using test images as shown in Fig. 4. An experiment was

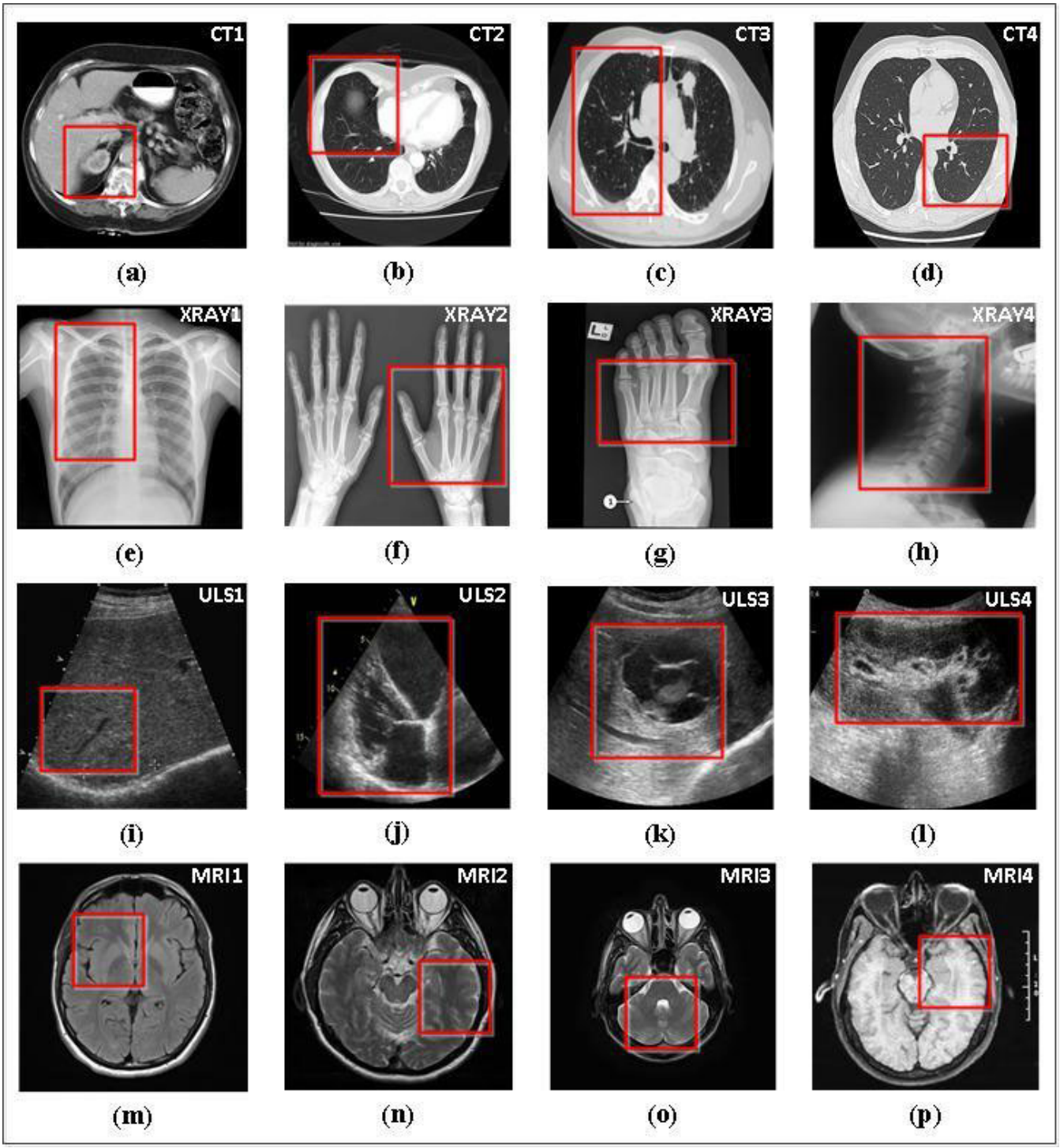

FIGURE 5. ROI selected on different medical images used in simulations.

carried out to test how efficiently the watermark information was implanted into the cover image. To have better watermarking scheme, it is necessary for the watermarked image to have the same visibility with the original one. Thus, for checking the visibility of the watermarked image, the values of PSNR and SSIM are calculated. The PSNR is defined using mean square error (MSE). The MSE is given in Eq. 6.

$$MSE = \frac{\sum_{M,N} [I(m,n) - I^w(m,n)]^2}{M \times N} \tag{6}$$

In Eq. 6 $I(m,n)$ is the original image and $I^w(m,n)$ is the watermarked of size $M \times N$, respectively. The formula for the

PSNR using MSE is given in Eq. 7. The PSNR is measured in decibels (dB) [4].

$$PSNR = 10\log_{10}\frac{R^2}{MSE} \tag{7}$$

The formula used for calculating SSIM is given in Eq. 8 and Eq. 9.

$$SSIM(I, I^w) = l(I, I^w)c(I, I^w)s(I, I^w) \tag{8}$$

$$l(I, I^w) = \frac{2\mu_x\mu_y + C1}{\mu_x^2 + \mu_y^2 + C1}$$

$$l(I, I^w) = \frac{2\sigma_x\sigma_y + C2}{\sigma_x^2 + \sigma_y^2 + C2}$$

$$l(I, I^w) = \frac{\sigma_{xy} + C3}{\sigma_x\sigma_y + C3} \tag{9}$$

In Eq. 8, the term 'l' represents luminance. It is actually the measure of comparison of luminance between the cover and watermarked image. If the luminance between the original and the watermarked image is the same, then the value of 'l' is considered as 1. In that case $\mu_x = \mu_y$. The term 'c' represents the contrast. It is the measure of contrast between the original and watermarked image. If the contrast between the host and the watermarked image is the same, then the value of 'c' is considered as 1. The term 's' in Eq. 8 represents the structural comparison. It is actually the measurement of correlation coefficient between the original and watermarked image. In Eq. 9, σ_x and σ_y are standard deviation and σ_{xy} is the covariance parameters of the respective images.

The PSNR and SSIM values are given in Table 2. The average PNSR for all test images is 44.0567 dB, whereas average SSIM is 0.9800. The results shown in Table 2 reveal that almost all test images have PSNR value more than 43 dB except two ultrasound images ULS3 and UL4 which have 42.5924 dB and 42.3355 dB, respectively, due to having high complex texture in the image. As described by Hajjaji [47], in medical image watermarking, the watermarking scheme is considered better if the imperceptibility of the watermarked image is equal or greater than 40 dB. The proposed scheme gives high imperceptibility of the marked images when two watermarks logo and EPR are implanted in the medical image. Similarly, the SSIM values given in Table 2 are more than 0.97 and thus are close to 1, indicating that the proposed technique gives high visual quality of watermarked images. The PSNR and SSIM values for XRAY1 image with different thresholds are shown in Table 3.

TABLE 2. Watermarked images showing values Of PSNR and SSIM.

Image Name	PSNR	SSIM
CT1	43.1564	0.9845
CT2	43.6261	0.9791
CT3	43.4607	0.9789
CT4	43.5717	0.9793
XRAY1	43.1658	0.9820
XRAY2	44.4668	0.9803
XRAY3	43.2723	0.9813
XRAY4	43.6407	0.9803
ULS1	43.1447	0.9798
ULS2	47.1771	0.9763
ULS3	42.5924	0.9840
ULS4	42.3355	0.9782
MRI1	44.2260	0.9774
MRI2	46.2831	0.9798
MRI3	46.2235	0.9800
MRI4	44.5647	0.9796
Average	44.0567	0.9800

TABLE 3. PSNR and SSIM values for watermarked images for Xray1 image at different thresholds.

T	PSNR	SSIM	T	PSNR	SSIM
10	47.5219	0.9969	60	42.0213	0.9775
20	46.6372	0.9941	70	41.0033	0.9735
30	45.5162	0.9904	80	40.0558	0.9700
40	44.3335	0.9863	90	39.2338	0.9668
50	43.1658	0.9820	100	38.3963	0.9636

Moreover, the performance of the proposed technique is compared with current medical image watermarking schemes [42], [43], [50], [51] in terms of average PSNR and SSIM values, as seen in Table 4. The bar graph shown in Fig. 6 also shows the comparison of the average value of PSNR of the proposed scheme with the average values of PSNR [42], [43], [50], [51].

TABLE 4. Comparison of proposed scheme with existing techniques with respect to PSNR and SSIM.

Scheme	PSNR	SSIM
Proposed	44.0567	0.9800
Lei et. al.[51]	41.5525	0.9660
Liu, Xiyao et. al. [42]	41.2995	0.9607
Thabit et. al. [43]	40.1841	0.9607
Maheshkar et. al. [50]	39.7522	0.9669

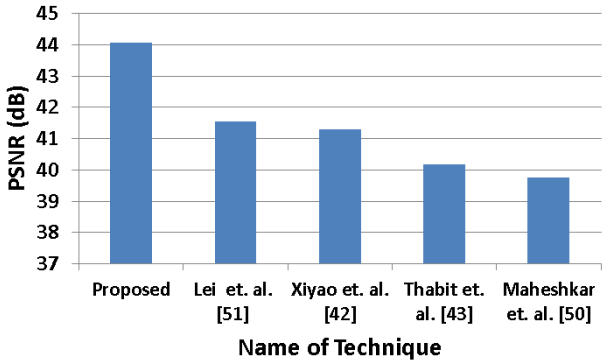

FIGURE 6. The comparison of proposed watermarking technique with the existing techniques.

C. ROBUSTNESS ANALYSIS

In order to analyze the robustness of the proposed scheme, different attacks were launched against watermarked images, such as noise attacks, filtering attacks, image compression, histogram equalization and resizing. The embedded watermarks are then extracted from these noisy images at the

receiving end. The normalized correlation coefficient (NCC) and BER are used to evaluate the robustness against these attacks. In addition, the proposed scheme is compared with the current state-of-art techniques [40], [48]. The performance of the proposed technique and the comparison analysis of the proposed technique with existing techniques are given in the following subsections. The formula used for BER is given in Eq. 10, whereas the formula for calculating NCC is given in Eq. 11.

$$BER(w, w^*) = \frac{\sum_{x=1}^{N}\sum_{y=1}^{N} w(x,y) \otimes w*(x,y)}{N^2} \tag{10}$$

In Eq. 5, w and w^* are the original and extracted watermarks and N is their size.

$$NCC = \frac{\sum_{x=1}^{N}\sum_{y=1}^{N} (w_{xy} - \mu_1) \times (w^*_{xy} - \mu_2)}{\sqrt{\sum_{x=1}^{N}\sum_{y=1}^{N} (w_{xy} - \mu_1)}\sqrt{\sum_{x=1}^{N}\sum_{y=1}^{N} (w^*_{xy} - \mu_2)}} \tag{11}$$

In Eq. 11, the $\mu_1 = \frac{1}{N^2}\sum_{x=1}^{N}\sum_{y=1}^{N} w_{xy}$ and $\mu_2 = \frac{1}{N^2}\sum_{x=1}^{N}\sum_{y=1}^{N} w^*_{xy}$

1) SALT AND PEPPER NOISE

The Salt and pepper noise attack was set against the watermarked images. The noise densities (ND) equal to 0.001, 0.003 and 0.005 are considered for this attack. After then the embedded watermark was extracted by applying the proposed algorithm. Table 5 shows the results.

TABLE 5. NCC and BER values for extracted logo and EPR under salt & pepper noise attack.

Medical Image	Logo		EPR	
	BER	NCC	BER	NCC
Density = 0.001				
CT1	0.0078	0.9836	0.0107	0.9707
XRAY1	0.0049	0.9897	0.0009	0.9844
ULS1	0.0088	0.9816	0.0078	0.9688
MRI1	0.0078	0.9836	0.0078	0.9649
Average	0.0073	0.9846	0.0068	0.9722
Density = 0.003				
CT1	0.0137	0.9712	0.0205	0.9590
XRAY1	0.0068	0.9858	0.0068	0.9863
ULS1	0.0176	0.9633	0.0195	0.9609
MRI1	0.0166	0.9653	0.0186	0.9629
Average	0.0136	0.9714	0.0163	0.9672
Density = 0.005				
CT1	0.0234	0.9507	0.0322	0.9357
XRAY1	0.0117	0.9756	0.0225	0.9551
ULS1	0.0264	0.9447	0.0322	0.9336
MRI1	0.0254	0.9467	0.0342	0.9316
Average	0.0217	0.9544	0.0302	0.9390

The results presented in Table 5 show that both BER and NCC values are close to 0 and 1 respectively, revealing the robustness of the proposed technique against the Salt and Pepper noise attack. The visual quality of the logo extracted from XRAY1 image when it underwent salt and pepper noise attack with different noise densities is shown in Fig. 7.

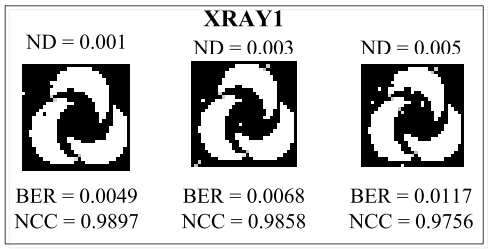

FIGURE 7. Extracted logo from noisy watermarked XRAY1 medical image.

Table 6 and Fig. 8 compare the performance of the proposed technique with existing medical image watermarking schemes [42], [50] under Salt and Pepper noise attack using average values of NCC in and in this case, the values of noise density chosen are 0.001, 0.003 and 0.005.

TABLE 6. Comparison Of the proposed scheme in terms of NCC with existing techniques under salt & pepper noise attack.

ND	Proposed (average)	Xiyao et. al. [42]	Maheshkar et. al. [50]
	NCC	NCC	NCC
0.001	0.9846	0.9744	0.9791
0.003	0.9714	0.9306	0.9642
0.005	0.9544	0.8866	0.9493

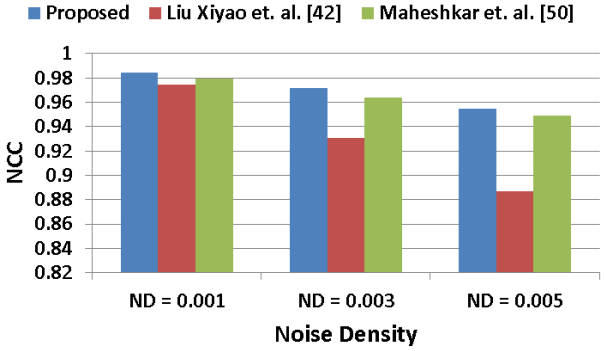

FIGURE 8. Comparison with the existing techniques under salt & pepper noise attack with different densities.

2) GAUSSIAN NOISE

The Gaussian noise attack was applied on watermarked images. The noise densities in this case were considered as 0.001, 0.003 and 0.005. After applying the Gaussian noise attack, the implanted watermark was extracted from the noisy images after applying the proposed technique. The analysis of CT scan, X-ray, Ultrasound and MRI images is given in Table 7.

TABLE 7. NCC and BER values of extracted logo and EPR under gaussian noise attack.

Medical Image	Logo		EPR	
	BER	NCC	BER	NCC
Variance = 0.001				
CT1	0.0000	1.0000	0.0000	1.0000
XRAY1	0.0000	1.0000	0.0009	0.9979
ULS1	0.0000	1.0000	0.0000	1.0000
MRI1	0.0000	1.0000	0.0000	1.0000
Average	0.0000	1.0000	0.0002	0.9994
Variance = 0.003				
CT1	0.0029	0.9938	0.0107	0.9785
XRAY1	0.0137	0.9715	0.0234	0.9532
ULS1	0.0146	0.8136	0.0137	0.9727
MRI1	0.0166	0.9652	0.0156	0.9688
Average	0.0119	0.9360	0.0158	0.9683
Variance = 0.005				
CT1	0.0215	0.9549	0.0303	0.9394
XRAY1	0.0420	0.9129	0.0615	0.8769
ULS1	0.0469	0.9018	0.0479	0.9044
MRI1	0.0498	0.8956	0.0469	0.9063
Average	0.0400	0.9163	0.0466	0.9067

The results of Table 7 show that both BER and NCC values are close to 0 and 1 respectively, showing the robustness of the proposed technique.

The visual quality and BER and NCC values of the extracted logo for CT1 image are shown in Fig. 9. For this attack, the variances of 0.001, 0.003, and 0.005 are selected.

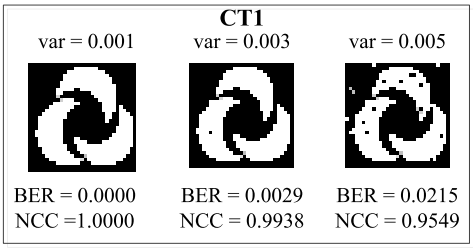

FIGURE 9. Extracted logo from noisy watermarked medical image CT1 when Gaussian Noise attack was applied with different variances.

The performance of the proposed technique is compared with current medical image watermarking schemes [42], [50] under Gaussian noise attack, as seen in Table 8 and Fig. 10. In this case, the average values of NC are selected for the proposed scheme using the variance values of 0.001, 0.003 and 0.005.

TABLE 8. Comparison of proposed scheme in terms of NCC with existing techniques under gaussian noise attack.

Density	Proposed	Xiyao et. al. [42]	Maheshkar et. al. [50]
	NCC	NCC	NCC
0.001	1.000	0.9885	0.9273
0.003	0.9360	0.9016	0.9268
0.005	09163	0.8723	0.9260

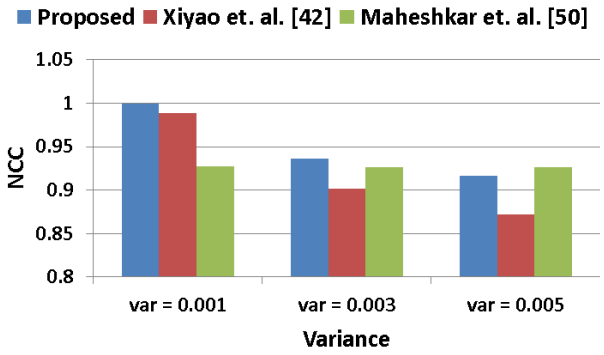

FIGURE 10. Comparison with other techniques under gaussian noise attack.

3) AVERAGE FILTERING

The proposed algorithm performed better in protecting watermark content when watermarked medical image went through average filter with window size of 3×3, 5×5 and 7×7. The BER and NCC values computed from the proposed algorithm are very close to ideal values and are presented in Table 9.

TABLE 9. NCC and BER values for extracted logo and EPR under average filtering attack.

Medical Image	Logo		EPR	
	BER	NCC	BER	NCC
Window = [3 × 3]				
CT1	0.0000	1.0000	0.0000	1.0000
XRAY1	0.0000	1.0000	0.0009	0.9979
ULS1	0.0000	1.0000	0.0000	1.0000
MRI1	0.0000	1.0000	0.0000	1.0000
Average	0.0000	1.0000	0.0002	0.9994
Window = [5 × 5]				
CT1	0.0029	0.9938	0.0107	0.9785
XRAY1	0.0137	0.9715	0.0234	0.9532
ULS1	0.0146	0.8136	0.0137	0.9727
MRI1	0.0166	0.9652	0.0156	0.9688
Average	0.0119	0.9360	0.0158	0.9683
Window = [7 × 7]				
CT1	0.0215	0.9549	0.0303	0.9394
XRAY1	0.0420	0.9129	0.0615	0.8769
ULS1	0.0469	0.9018	0.0479	0.9044
MRI1	0.0498	0.8956	0.0469	0.9063
Average	0.0400	0.9163	0.0466	0.9067

The visual quality of the extracted logo with BER and NCC values for ULS1 is shown in Fig. 11. The window sizes of 3×3 and 5×5 are selected for this experiment.

The performance comparison analysis of the proposed technique with current techniques [42], [50] under Average Filtering attack is presented in Table 10 and Fig. 12. In this case window sizes of 3×3 and 5×5 are chosen.

4) MEDIAN FILTERING

The proposed algorithm also performed better in protecting watermark content when watermarked medical image underwent Median Filtering attack. The BER and NCC values computed after applying the proposed algorithm are very

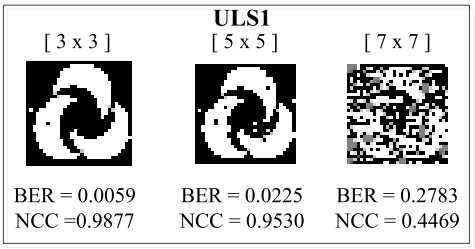

FIGURE 11. Extracted logo from noisy watermarked medical image ULS1, when average filtering attack was applied with different window sizes.

TABLE 10. Comparison of proposed scheme in terms of NCC with existing techniques under average filtering attack.

Window Size	Proposed	Liu Xiyao et. al. [42]	Maheshkar et. al. [50]
	NCC	NCC	NCC
3× 3	0.9754	0.9604	0.8868
5× 5	0.8595	0.8978	0.7831

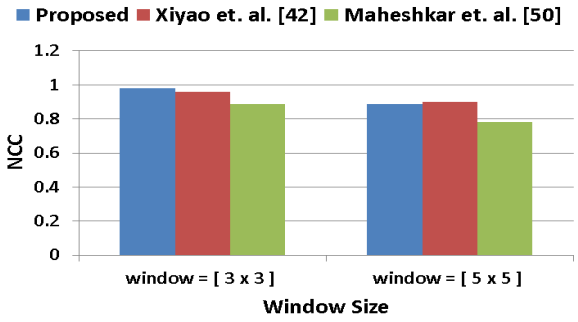

FIGURE 12. Comparison with the current schemes under average filtering attack with different window sizes.

close to the ideal values when window sizes of 3 × 3 and 5 × 5 are used. However, for window size of 7 × 7, the proposed scheme survived marginally. The results of BER and NCC are given in Table 11.

BER and NCC values of retrieved logo along with visual quality under different window sizes for MRI1 medical image are shown in Fig. 13. The window sizes of 3 × 3 and 5 × 5 and 7 × 7 are chosen for analyzing this attack.

The performance comparison analysis of the proposed technique with current medical image watermarking techniques [42], [50] under Median Filtering attack is seen in Table 12 and Fig. 14. In this case window sizes of 3 × 3 and 5 × 5 are chosen.

5) GAUSSIAN BLURRING

The proposed algorithm had good performance in protecting watermark content when watermarked medical image went through Gaussian Blurring attack. The BER and NCC values computed after applying the proposed algorithm are exactly equal to the ideal value of 0 and 1 when the value of sigma is chosen as 0.5 for Gaussian Blur attack. However, the values of BER and NCC are close to ideal values when the value

TABLE 11. NCC and BER values for extracted watermarks under median filtering attack with different window sizes.

Medical Image	Logo		EPR	
	BER	NCC	BER	NCC
Window = [3 × 3]				
CT1	0.0039	0.9918	0.0088	0.9824
XRAY1	0.0029	0.9939	0.0029	0.9942
ULS1	0.0039	0.9918	0.0029	0.9941
MRI1	0.0009	0.9979	0.0049	0.9902
Average	0.0029	0.9938	0.0048	0.9902
Window = [5 × 5]				
CT1	0.0566	0.8818	0.0352	0.9298
XRAY1	0.0361	0.9245	0.0516	0.9688
ULS1	0.0137	0.9715	0.0186	0.9629
MRI1	0.0098	0.9795	0.0098	0.9805
Average	0.0290	0.9393	0.0288	0.9605
Window = [7 × 7]				
CT1	0.2471	0.4989	0.1250	0.7502
XRAY1	0.2041	0.5819	0.0918	0.8164
ULS1	0.1670	0.6597	0.0537	0.8927
MRI1	0.1523	0.6882	0.0195	0.9609
Average	0.1926	0.6071	0.0725	0.8550

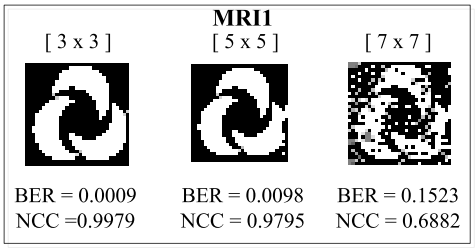

FIGURE 13. Extracted logo from noisy watermarked medical image, MRI1, when median filtering attack was applied on the image with different window sizes.

TABLE 12. Comparison of proposed scheme in terms of NCC with existing techniques under median filtering attack.

Window Size	Proposed	Xiyao et. al. [42]	Maheshkar et. al. [50]
	NCC	NCC	NCC
3 x 3	0.9938	0.9759	0.9115
5 x 5	0.9393	0.9215	0.7934

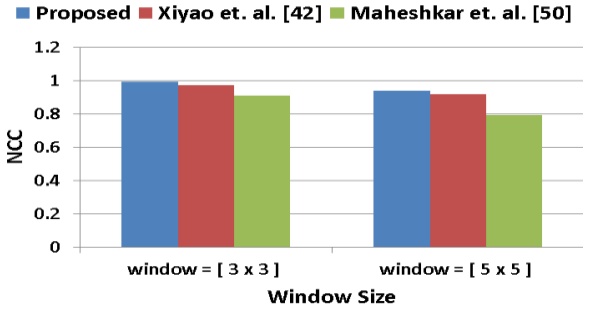

FIGURE 14. Comparison of proposed technique under median filtering attack with different window sizes.

of sigma is chosen as 1. The values of BER and NCC in the test images of CT1, XRAY1, ULS1 and MRI1 are presented in Table 13.

TABLE 13. NCC and BER values for extracted logo and EPR under gaussian blur attack.

Medical Image	Logo		EPR	
	BER	NCC	BER	NCC
Sigma= 0.5				
CT1	0	1	0	1
XRAY1	0	1	0	1
ULS1	0	1	0	1
MRI1	0	1	0	1
Average	0	1	0	1
Sigma = 1.0				
CT1	0.0215	0.9551	0.0146	0.9708
XRAY1	0.0127	0.9733	0.0059	0.9883
ULS1	0.0059	0.9877	0.0088	0.9824
MRI1	0.0059	0.9877	0.0059	0.9883
Average	0.0115	0.9749	0.0088	0.9824

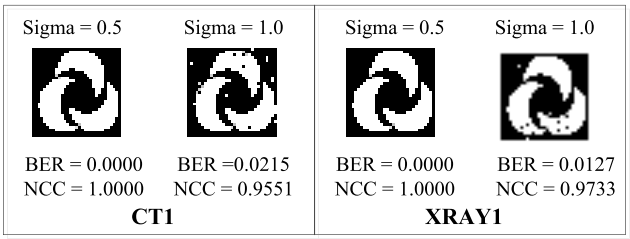

FIGURE 15. Extracted logo from noisy watermarked medical images CT1 and XRAY1 when gaussian blurring attack was applied on watermarked images with different values of Sigma.

TABLE 14. Comparison of proposed scheme in terms of NCC with existing techniques under gaussian blurring attack.

Sigma	Proposed	Xiyao et. al. [42]	Maheshkar et. al. [50]
	NCC	NCC	NCC
0.5	1.0000	0.9937	0.9797
1.0	0.9749	0.9422	0.8733

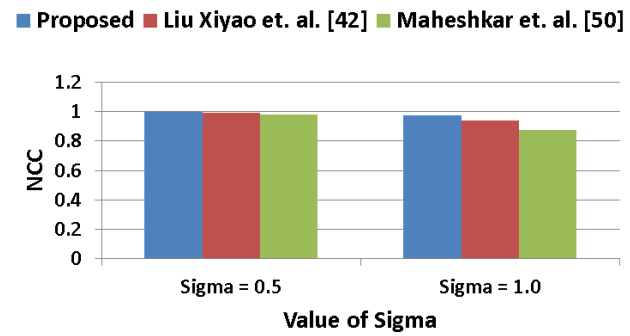

FIGURE 16. Comparison of the proposed technique with existing techniques under gaussian blurring attack.

The visual quality of the extracted logo along with BER and NCC values for both CT1, and XRAY1 medical images is shown in Fig. 15.

The performance of the proposed technique is compared with the current techniques [42], [50] under Gaussian Blurring attack, as shown in Table 14 and Fig. 16.

6) JPEG COMPRESSION

The proposed algorithm had super performance in protecting watermark content when watermarked medical image underwent JPEG compression attack. The BER and NCC values computed after applying the proposed algorithm are equal to ideal values and are shown in Table 15. The Quality Factors (QF) used for compressing the watermarked images are selected as 60, 70, 80 and 90.

TABLE 15. NCC and BER values for extracted watermarks under jpeg compression attack.

Medical Image	Logo		EPR	
	BER	NCC	BER	NCC
QF = 60				
CT3	0.0000	1.0000	0.0000	1.0000
XRAY3	0.0000	1.0000	0.0000	1.0000
ULS3	0.0000	1.0000	0.0000	1.0000
MRI3	0.0000	1.0000	0.0000	1.0000
Average	0.0000	1.0000	0.0000	1.0000
QF = 70				
CT3	0.0000	1.0000	0.0000	1.0000
XRAY3	0.0000	1.0000	0.0000	1.0000
ULS3	0.0000	1.0000	0.0000	1.0000
MRI3	0.0000	1.0000	0.0000	1.0000
Average	0.0000	1.0000	0.0000	1.0000
QF = 80				
CT3	0.0000	1.0000	0.0000	1.0000
XRAY3	0.0000	1.0000	0.0000	1.0000
ULS3	0.0000	1.0000	0.0000	1.0000
MRI3	0.0000	1.0000	0.0000	1.0000
Average	0.0000	1.0000	0.0000	1.0000
QF = 90				
CT3	0.0000	1.0000	0.0000	1.0000
XRAY3	0.0000	1.0000	0.0000	1.0000
ULS3	0.0000	1.0000	0.0000	1.0000
MRI3	0.0000	1.0000	0.0000	1.0000
Average	0.0000	1.0000	0.0000	1.0000

The extracted logo from noisy watermarked medical image CT3 after JPEG Compression attack with Quality Factors: 60, 70, 80, and 90 is shown in Figure 17. The performance comparison analysis of the proposed scheme with current medical image watermarking techniques [42], [50] under JPEG compression attack is shown in Table 16 and Fig. 18. In this case, Quality Factors 70 and 80 are chosen for the comparison.

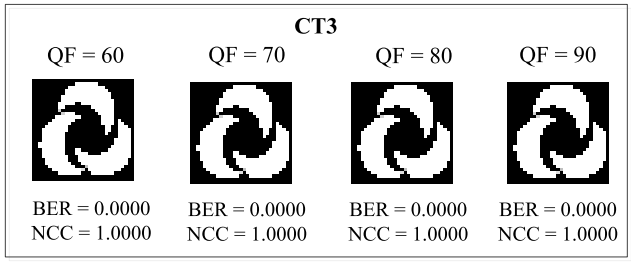

FIGURE 17. Extracted logo from noisy watermarked medical image CT3 after JPEG compression attack with different quality factors: (QF = 60, 70, 80, 90).

7) JPEG2000 COMPRESSION

Our algorithm delivers super performance in protecting watermark content when watermarked medical image was under JPEG2000 compression attack. The BER and NCC

TABLE 16. Comparison of proposed scheme in terms of NCC with existing techniques under jpeg compression attack.

QF	Proposed	Xiyao et. al. [42]	Maheshkar et. al. [50]
	NCC	NCC	NCC
70	1	0.9939	0.9700
80	1	0.9982	0.9721

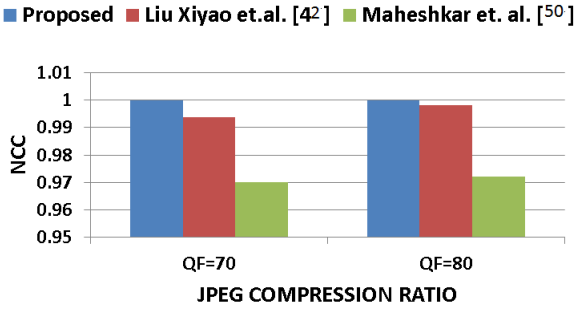

FIGURE 18. Comparison with the current techniques under JPEG compression attack.

TABLE 17. NCC and BER values for extracted logo and EPR under Jpeg2000 compression attack.

Medical Image	Logo		EPR	
	BER	NCC	BER	NCC
CR = 4				
CT4	0.0000	1.0000	0.0000	1.0000
XRAY4	0.0000	1.0000	0.0000	1.0000
ULS4	0.0000	1.0000	0.0000	1.0000
MRI4	0.0000	1.0000	0.0000	1.0000
Average	0.0000	1.0000	0.0000	1.0000
CR = 5				
CT4	0.0000	1.0000	0.0000	1.0000
XRAY4	0.0000	1.0000	0.0000	1.0000
ULS4	0.0000	1.0000	0.0000	1.0000
MRI4	0.0000	1.0000	0.0000	1.0000
Average	0.0000	1.0000	0.0000	1.0000
CR = 8				
CT4	0.0000	1.0000	0.0000	1.0000
XRAY4	0.0000	1.0000	0.0000	1.0000
ULS4	0.0000	1.0000	0.0000	1.0000
MRI4	0.0000	1.0000	0.0000	1.0000
Average	0.0000	1.0000	0.0000	1.0000
CR = 9				
CT4	0.0000	1.0000	0.0000	1.0000
XRAY4	0.0000	1.0000	0.0000	1.0000
ULS4	0.0000	1.0000	0.0000	1.0000
MRI4	0.0000	1.0000	0.0000	1.0000
Average	0.0000	1.0000	0.0000	1.0000

values computed after applying the proposed algorithm are equal to ideal values and are given in Table 17. The Compression Ratios (CR) 4, 5, 8, 9 are chosen for compressing the watermarked medical images, CT4, XRAY4, ULS4 and MRI4.

The visual quality of the extracted watermark along with BER and NCC values under different values of CR for XRAY4 medical image is depicted in Fig. 19. For this experiment, CR of 4, 5, 8 and 9 are chosen.

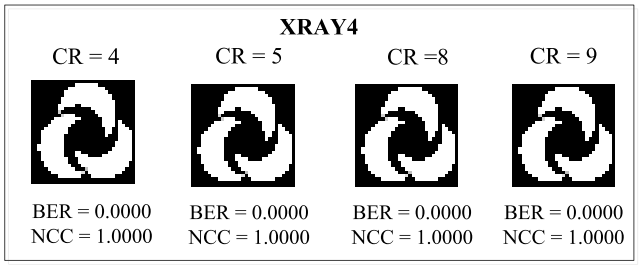

FIGURE 19. Extracted logo from noisy watermarked medical image XRAY4 after JPEG2000 compression attack with different compression ratio (CR = 4, 5, 8, 9).

The performance of the proposed technique is compared with existing techniques [42], [50] under JPEG2000 compression attack, as seen in Table 18 and Fig. 20. In this case, CR values of 4 and 8 are chosen for the comparison.

TABLE 18. Comparison of the proposed scheme in terms of NCC with existing techniques under Jpeg2000 compression attack.

CR	Proposed	Xiyao et. al. [42]	Maheshkar et. al. [50]
	NCC	NCC	NCC
4	1	0.9993	0.9755
8	1	0.9874	0.9539

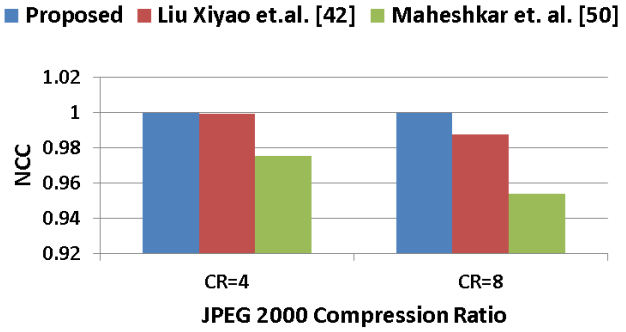

FIGURE 20. Comparison of proposed technique with the existing techniques under JPEG2000 compression attack with different values of CR.

8) HISTOGRAM EQUALIZATION

The proposed algorithm had good performance in protecting watermark content when watermarked medical image was under Histogram Equalization attack. The BER and NCC values computed after applying the proposed algorithm are equal to ideal values in the case of CT1 and MRI1 medical images; whereas in the case of XRAY1 and ULS1, the BER and NCC are close to ideal values. The computed BER and NCC values are shown in Table 19.

The visual quality of the extracted logo along with BER and NCC values for CT1, XRAY1, ULS1 and MRI1 medical image is shown in Fig. 21.

TABLE 19. NCC and BER values for extracted watermarks under histogram equalization attack.

Medical Image	Logo		EPR	
	BER	NCC	BER	NCC
CT1	0	1	0	1
XRAY1	0.0127	0.9734	0.0127	0.9748
ULS1	0.0029	0.9938	0.0039	0.9922
MRI1	0.0000	1.0000	0.0020	0.9961
Average	0.0039	0.9918	0.0046	0.9907

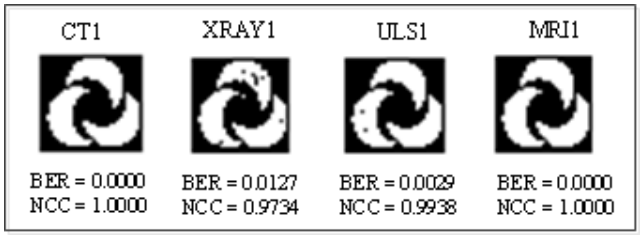

FIGURE 21. Extracted logo from noisy watermarked medical images CT1, XRAY1, ULS1 and MRI1 after histogram equalization attack on watermarked medical images.

TABLE 20. Comparison of proposed scheme in terms of NCC with existing techniques under histogram equalization attack.

Image	Proposed	Liu Xiyao et. al. [42]	Maheshkar et. al. [50]
	NCC	NCC	NCC
Average	0.9918	N/A	0.8950

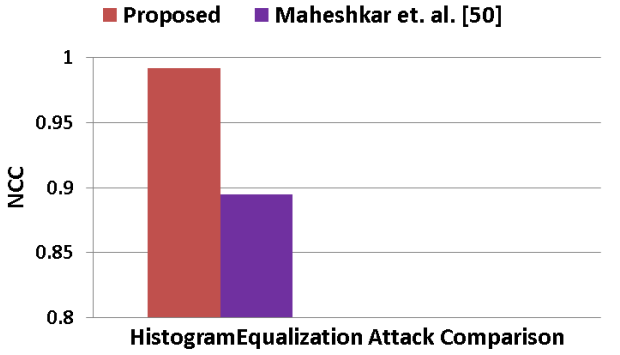

FIGURE 22. Comparison of average value of NC for four cover images for the proposed technique with the existing techniques under histogram equalization attack.

The performance comparison of the proposed technique using the average NC value of four cover images (CT1, XRAY1, ULS1 and MRI1) with the average value of NCC reported by existing medical image watermarking schemes [40], [48] under Histogram Equalization attack is given in Table 20 and Fig. 22. Since the watermarked technique presented by Xiyao *et al.* [40] has not reported the NCC values for Histogram Equalization Attack, we compared our results with the scheme proposed by Maheshkar et. al. [48] for Histogram Equalization attack.

9) RESIZING

The proposed algorithm had good performance in protecting watermark content when watermarked medical image underwent Resizing attack. The BER and NCC values computed after applying the proposed algorithm was close to ideal values when the proposed algorithm was applied on CT1, XRAY1, ULS1 and MRI1 medical images. The computed BER and NCC values are shown in Table 21.

TABLE 21. NCC and BER values for extracted logo and EPR under resizing attack.

Medical Image	Logo		EPR	
	BER	NCC	BER	NCC
RS(0.5)				
CT1	0	1	0.0039	0.9922
XRAY1	0.0049	0.9897	0.0029	0.9941
ULS1	0.0039	0.9918	0.002	0.9961
MRI1	0	1	0	1
Average	0.0022	0.9953	0.0022	0.9956
RS(0.8)				
CT1	0.0059	0.9878	0.0009	0.998
XRAY1	0.0127	0.9809	0.0029	0.9941
ULS1	0.0029	0.9939	0.0029	0.9941
MRI1	0	1	0.0009	0.998
Average	0.0053	0.9906	0.0019	0.9960
RS(1.2)				
CT1	0	1	0	1
XRAY1	0	1	0	1
ULS1	0	1	0	1
MRI1	0	1	0	1
Average	0	1	0	1

The visual quality of the extracted logo along with BER and NCC values for XRAY1 medical image is shown in Fig. 23.

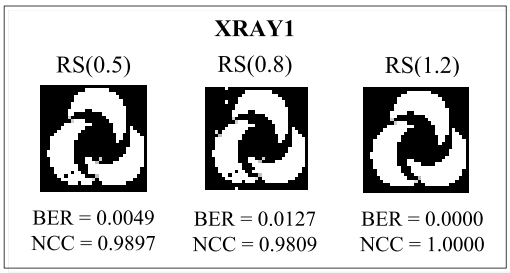

FIGURE 23. Extracted logo from noisy watermarked medical image XRAY1 after resizing attack.

The comparison performance of the proposed technique using the average NC values of four cover images CT1, XRAY1, ULS1 and MRI1 with the average value of NC reported by existing medical image watermarking schemes [40], [48] under the Resizing attack is shown in Table 22 and Fig. 24. The results shown in Table 22 and Fig. 24 reveal that the proposed algorithm gives better results than that of Maheshkar [50] for both scaling factors of 0.8 and 1.2. However, for Liu *et al.* [42], it reports a better result with a scaling factor of 1.2, but it is marginally lower with a scaling factor of 0.8.

TABLE 22. Comparison of proposed scheme in terms of NCC with existing techniques under resizing attack.

RS	Proposed	Xiyao et. al. [42]	Maheshkar et. al. [50]
	NCC	NCC	NCC
RS(0.8)	0.9906	0.9972	0.9683
RS(1.2)	1	0.9988	0.9906

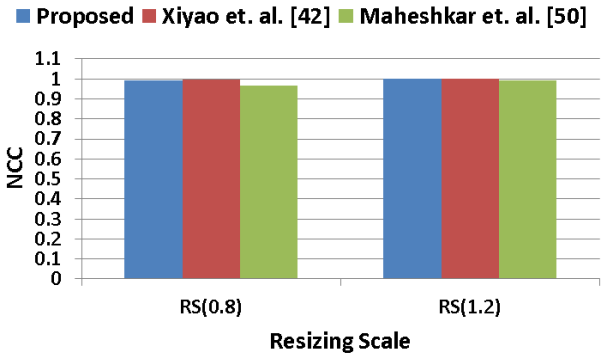

FIGURE 24. Comparison of average value of NC of four cover images with the existing techniques under resizing attack.

10) CROPPING

The proposed algorithm had good performance in protecting watermark content when watermarked medical image underwent Cropping attack. The BER and NCC values computed after applying the proposed algorithm was close to ideal values when the proposed algorithm was applied on CT1, XRAY1, ULS1 and MRI1 medical images. The computed BER and NCC values are shown in Table 23.

TABLE 23. NCC and BER values for extracted logo and EPR under resizing attack.

Medical Image	Logo		EPR	
	BER	NCC	BER	NCC
CRP(5% Y axis)				
CT1	0	1	0	1
XRAY1	0.0127	0.9735	0.0215	0.9579
ULS1	0.0127	0.9735	0.0234	0.9542
MRI1	0.0166	0.9654	0.0273	0.9468
Average	0.0105	0.9781	0.0180	0.9647
CRP(8% Y axis)				
CT1	0	1	0	1
XRAY1	0.0332	0.9514	0.0459	0.9121
ULS1	0.0273	0.9434	0.0381	0.9266
MRI1	0.0303	0.9374	0.0449	0.9139
Average	0.0227	0.9581	0.0322	0.9381
CRP(20% Y axis)				
CT1	0.0117	0.9755	0.0127	0.9749
XRAY1	0.0752	0.8476	0.1143	0.7929
ULS1	0.0859	0.8260	0.1016	0.8142
MRI1	0.0869	0.8247	0.1094	0.8010
Average	0.0649	0.8685	0.0845	0.8457

The visual quality of the extracted logo along with BER and NCC values for XRAY1 medical image is shown in Fig. 25.

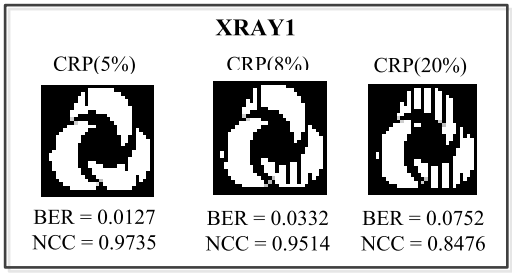

FIGURE 25. Extracted logo from noisy watermarked medical image XRAY1 after cropping attack.

TABLE 24. Comparison of proposed scheme in terms of NCC with existing techniques under cropping attack.

CRP	Proposed	Yuan et. al. [52]	Zear et. al. [38]
	NCC	NCC	NCC
CRP(8% Yaxis)	0.9581	0.9400	0.7900

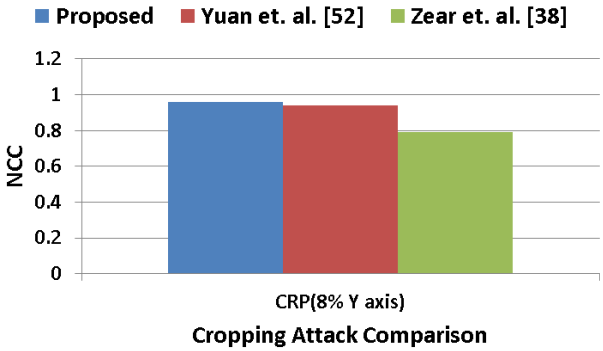

FIGURE 26. Comparison of average value of NC of four cover images with the existing techniques under cropping attack.

The comparison performance of the proposed technique using the average NC values of four cover images CT1, XRAY1, ULS1 and MRI1 with the average value of NC reported by existing medical image watermarking schemes [36], [50] under the Cropping attack is shown in Table 24 and Fig. 25. The results shown in Table 24 and Fig. 25 reveal that the proposed algorithm gives better results than that of Zear el. al [36] for and Yuan *et al.* [50] for Cropping with (8% Y axis)

D. PERFORMANCE COMPARISON OF THE PROPOSED SCHEME WITH OTHER SCHEMES

The performance comparison of the proposed technique with other techniques currently reported in the literature [51], [52] in terms of NCC is given in Table 25. The XRAY1 medical image is used for this comparison analysis. Singh *et al.* [51] and Parah *et al.* [52] also reported their BER and NCC values for the same XRAY1 image.

Table 25 reveals that proposed technique outperformed the existing techniques [51], [52] by withstanding against all types of attacks which are considered for analysis.

TABLE 25. Comparison analysis of the proposed technique with existing techniques under different attacks using NCC values of extracted logo.

Attack sequence	Attacks	Proposed	Singh et. al.[53]	Parah et. al.[54]
		Logo (NCC)	Logo (NCC)	Logo (NCC)
1.	Gaussian Noise (var=0.01)	0.7887	0.7394	0.1456
2.	Gaussian Noise (var=0.05)	0.4276	0.6994	0.0334
3.	Salt & Pepper Noise (d=0.02)	0.8573	0.7394	0.5472
4.	Salt & Pepper Noise (d=0.05)	0.5079	0.7072	0.0928
5.	Median Filtering [2 x 2]	0.9795	0.6662	0..4393
6.	Median Filtering [3 x 3]	0.9939	0.2162	0.4367
7.	Histogram Equalization	0.9735	0.7402	0.9925
8.	JPEG (QF=50)	1	0.7364	0.9715
9.	JPEG (QF=70)	1	0.7394	0.9912
10.	JPEG (QF=90)	1	0.7394	0.9923
11.	Scaling (2)	1	0.7364	1
12	Scaling (2.5)	1	0.7364	1
13	Scaling (5)	1	0.7335	1

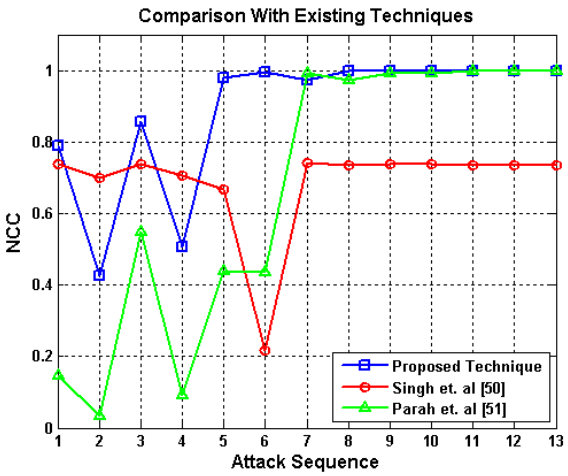

FIGURE 27. Comparison of the proposed scheme with some currently reported watermarking schemes on the basis of NCC values after applying different attacks.

Fig. 27 also shows that the proposed scheme outperformed the existing medical image watermarking schemes [51], [52].

Finally we compared the proposed technique with the technique recently reported by Kahlessename *et al.* [55]. The comparison shown in Table 26 and its corresponding bar graph shown in Figure 28. The Results shown in Table 26 and Figure 28 reveals that our proposed technique outperforms the technique [53].

TABLE 26. Comparison analysis of the proposed technique with existing techniques under different attacks using NCC values of extracted logo.

Attack sequence	Attacks	Proposed	Kahlessename et. al [55]
		(NCC)	(NCC)
1.	Histogram Equalization	0.9735	0.8555
2.	Average Filter	1.0000	0.9567
3.	Cropping	0.9735	0.5829
4.	JPEG Compression	1.0000	0.9617
5.	Salt & Pepper	0.9897	0.9617
6.	Scaling	1	0.7475

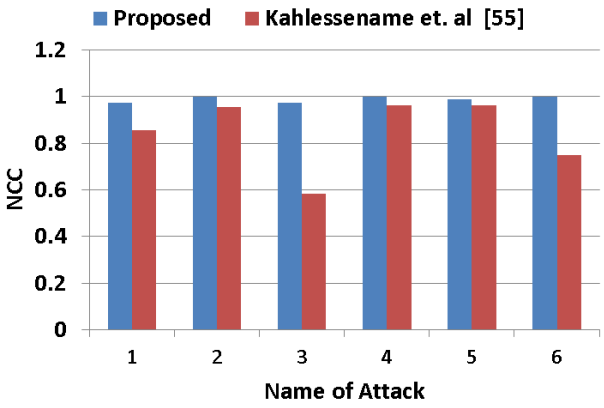

FIGURE 28. Comparison of the proposed scheme with recently reported watermarking schemes on the basis of NCC values after applying different attacks.

VI. CONCLUSION

A new blind and robust framework for watermarking of medical images has been presented. The scheme is a fusion of DCT, DWT and SVD transforms. Block-based LL sub-band of RONI area is exploited after applying the DWT on RONI area of input medical image. In order to increase the imperceptibility and robustness of the scheme, the singular values are used for implanting the watermark information after applying the SVD transform on DCT carrier matrices. To create a balance between the visual quality of the watermarked image and its robustness, an optimal threshold is selected for each set of medical images. Watermarks are extracted using the same key that was used at the time of embedding. Compared with current state-of-art watermark techniques, the proposed technique performs better in terms of imperceptibility and robustness. The pros and cons of the proposed technique are that it achieves higher rates of imperceptibility and robustness by combining three transforms DCT, DWT and SVD. However, due to fusion of these three transforms the computational complexity and potential threat of false positives are increased which can be addressed by future researchers.

REFERENCES

[1] N. A. Memon and A. Alzahrani, "Prediction-based reversible watermarking of CT scan images for content authentication and copyright protection," *IEEE Access*, vol. 8, pp. 75448–75462, Apr. 2020.

[2] A. Anand and A. K. Singh, "Watermarking techniques for medical data authentication: A survey," *Multimedia Tools Appl.*, vol. 22, no. 2, pp. 45–52, Apr. 2020.

[3] M. T. Ahvanooey, Q. Li, H. J. Shim, and Y. Huang, "A comparative analysis of information hiding techniques for copyright protection of text documents," *Hindawi Secur. Commun. Netw.*, vol. 2018, pp. 1–22, Apr. 2018.

[4] S. P. Mohanty, A. Sengupta, P. Guturu, and E. Kougianos, "Everything you want to know about watermarking: From paper marks to hardware protection," *IEEE Consum. Electron. Mag.*, vol. 6, no. 3, pp. 83–91, Jul. 2017

[5] U. Verma and N. Sharma, "Hybrid mode of medical image watermarking to enhance robusness and imperceptibility," *Int. J. Innov. Technol. Exploring Eng.*, vol. 9, no. 1, pp. 351–359, Nov. 2019.

[6] A. Rehman, K. Sultan, N. Aldhafferi, A. Alqahtiani, and M. Mahmood, "Reversible and fragile watermarking scheme for medical images," *Comput. Math. Methods Med.*, vol. 18, p. 7, Jul. 2018.

[7] A. F. Qasim, R. Aspin, F. Meziane, and P. Hogg, "ROI-based reversible watermarking scheme for ensuring the integrity and authenticity of DICOM MR images," *Multimedia Tools Appl.*, vol. 78, no. 12, pp. 16433–16463, Jun. 2019.

[8] S. M. Mousavi, A. Naghsh, and S. Abu-Bakar, "Watermarking techniques used in medical images: A survey," *J. Digit. Imag.*, vol. 27, no. 6, pp. 714–729, 2014.

[9] N. A. Memon, A. Chaudhry, M. Ahmad, and Z. A. Keerio, "Hybrid watermarking of medical images for ROI authentication and recovery," *Int. J. Comput. Math.*, vol. 88, no. 10, pp. 2057–2071, Jul. 2011.

[10] F. Abbasi and N. A. Memon, "Reversible watermarking for the security of medical image databases," in *Proc. 21st Saudi Comput. Soc. Nat. Comput. Conf. (NCC)*, Riyadh, Saudi Arabia, Apr. 2018, pp. 1–6.

[11] B. Hassan, R. Ahmed, B. Li, and O. Hassan, "An imperceptible medical image watermarking framework for automated diagnosis of retinal pathologies in an eHealth arrangement," *IEEE Access*, vol. 7, pp. 69758–69775, 2019.

[12] V. Kelkar, J. H. Mehta, and K. Tuckley, "A novel robust reversible watermarking technique based on prediction error expansion for medical images," in *Proc. 2nd Int. Conf. Comput. Vis. Image Process.*, in Advances in Intelligent Systems and Computing, vol. 703, 2018, pp. 131–143.

[13] W. Mazurczyk and S. Wndzel, "Information hiding: Chanllegnes for forensic experts," *Commun. ACM*, vol. 61, no. 1, pp. 86–94, 2018.

[14] S. Thakur, A. K. Singh, S. P. Ghreara, and M. Elhoseny, "Multilayer security of medical data through watermarking and chaotic encryption for telehealth applications," *Multimedia Tools Appl.*, vol. 78, no. 3, pp. 3457–4370, 2019.

[15] T. K. Al-Shayea, C. X. Mavromoustakis, J. M. Batalla, and G. Mastorakis, "A hyberidized methodology of different wavelet transforms targetting medical images in IoT infrastructure," *Measurement*, vol. 148, pp. 1–14, Jul. 2019.

[16] H. V. Singh and A. Rai, "Medical image watermarking in transformed domain," in *Smart Innovations in Communication and Computational Sciences*. Singapore: Springer, 2018, pp. 485–493.

[17] S. Sharma and V. Kumar, "A survey of blind and non-blind watermarking techniques," *Int. J. Sci. Eng. Res.*, vol. 7, no. 12, pp. 1218–1223, 2016.

[18] A. Shehab, M. Elhoseny, K. Muhammad, A. K. Sangaiah, P. Yang, H. Huang, and G. Hou, "Secure and robust fragile watermarking scheme for medical images," *IEEE Access*, vol. 6, pp. 10269–10278, 2018.

[19] A. K. Abdulrahman and S. Ozturk, "A novel hybrid DCT and DWT based robust watermarking algorithm for color images," *Multimedia Tools Appl.*, vol. 78, no. 12, pp. 17027–17049, Jan. 2019.

[20] N. Agarwal, A. K. Singh, and P. K. Singh, "Survey of robust and imperceptible watermarking," *Multimedia Tools Appl.*, vol. 78, no. 7, pp. 8603–8633, 2019.

[21] J. Liu, J. Li, J. Ma, U. N. Sadiq, and A. Yang, "A robust multi-watermarking algorithm for medical images based on DTCWT-DCT and Henon map," *Appl. Sci.*, vol. 9, no. 4, pp. 1–23, 2019.

[22] A. Rehman, K. Sultan, N. Aldhafferi, A. Alqahtiani, and M. Mahmood, "Reversible and fragile watermarking scheme for medical images," *Comput. Math. Methods Med.*, vol. 18, p. 7, Jul. 2018.

[23] N. A. Memon and S. A. M. Gilani, "Watermarking of chest CT scan medical images for content authentication," *Int. J. Comput. Math.*, vol. 88, no. 2, pp. 265–280, 2010.

[24] F. Cao, B. An, J. Wang, D. Ye, and H. Wang, "Hierarchical recovery for tampered images based on watermark self-embedding," *Displays*, vol. 46, pp. 52–60, Jan. 2017.

[25] H. Zhang, C. Wang, and X. Zhou, "Fragile watermarking for image authentication using the characteristic of SVD," *Algorithms*, vol. 10, no. 1, pp. 1–12, 2017.

[26] K. Konstantinides, B. Natarajan, and G. S. Yovanof, "Noise estimation and filtering using block-based singular value decomposition," *IEEE Trans. Image Process.*, vol. 6, no. 3, pp. 479–483, Mar. 1997.

[27] R. Liu and T. Tan, "An SVD-based watermarking scheme for protecting rightful ownership," *IEEE Trans. Image Process.*, vol. 6, no. 3, pp. 479–483, Aug. 1997.

[28] S. Roy and A. K. Pal, "An indirect watermark hiding in discrete cosine transform–singular value decomposition domain for copyright protection," *Roy. Soc. Open Sci.*, vol. 4, no. 6, 2017, Art. no. 170326.

[29] M.-Q. Fan, H.-X. Wang, and S.-K. Li, "Restudy on SVD-based watermarking scheme," *Appl. Math. Comput.*, vol. 203, no. 2, pp. 926–930, 2008.

[30] N. M. Makbol, B. E. Khoo, and T. H. Rassem, "Block-based discrete wavelet transform-singular value decomposition image watermarking scheme using human visual system characteristics," *IET Image Process.*, vol. 10, no. 1, pp. 34–52, 2016.

[31] V. Seenivasagam and R. Velumani, "A QR code based zero-watermarking scheme for authentication of medical images in teleradiology cloud," *Comput. Math. Methods Med.*, vol. 2013, pp. 1–16, 2013.

[32] A. K. Singh, M. Dave, and A. Mohan, "Hybrid technique for robust and imperceptible multiple watermarking using medical images," *Multimedia Tools Appl.*, vol. 75, no. 14, pp. 8381–8401, 2016.

[33] X. Zhou, H. Zhang, and C. Wang, "A robust image watermarking scheme based on DWT, APDCTBT and SVD," *Symmetry*, vol. 10, p. 77, Mar. 2018.

[34] S. B. B. Ahmadi, G. Zhang, S. Wei, and L. Boukela, "An intelligent and blind image watermarking scheme based on hybrid SVD transforms using human visual system characteristics," *Vis. Comput.*, vol. 37, no. 2, pp. 385–409, Feb. 2021.

[35] M. M. Soliman, A. E. Hassanien, N. I. Ghali, and H. M. Onsi, "An adaptive watermarking approach for medical imaging using swarm intelligent," *Int. J. Smart Home*, vol. 6, no. 1, pp. 37–50, 2012.

[36] A. Zear, A. K. Singh, and P. Kumar, "A proposed secure multiple watermarking technique based on DWT, DCT and SVD for application in medicine," *Multimedia Tools Appl*, vol. 77, no. 4, pp. 4863–4882, 2018.

[37] F. Ernawan, S.-C. Liew, Z. Mustaffa, and K. Moorthy, "A blind multiple watermarks based on human visual characteristics," *Int. J. Elect. Comput. Eng.*, vol. 8, no. 4, pp. 2578–2587, 2018.

[38] N. Alias and F. Ernawan, "Multiple watermarking technique using optimal threshold," *Indonesian J. Electr. Eng. Comput. Sci.*, vol. 18, no. 1, pp. 368–376, Apr. 2020.

[39] F. N. Thakkar and V. K. Srivastava, "A blind medical image watermarking: DWT-SVD based robust and secure approach for telemedicine applications," *Multimdia Tools Appl.*, vol. 76, pp. 3669–3697, Feb. 2017.

[40] X. Liu, J. Lou, H. Fang, Y. Chen, P. Ouyang, Y. Wang, B. Zou, and L. Wang, "A novel robust reversible watermarking scheme for protecting authenticity and integrity of medical images," *IEEE Access*, vol. 7, pp. 76580–76598, 2019.

[41] R. Thabit and B. E. Khoo, "Medical image authentication using SLT and IWT schemes," *Multimedia Tools Appl.*, vol. 76, no. 1, pp. 309–332, Jan. 2017.

[42] J. Dowling, B. M. Planitz, A. J. Maeder, J. Du, B. Pham, C. Boyd, S. Chen, A. P. Bradley, and S. Crozier, "A comparison of DCT and DWT block based watermarking on medical image quality," in *Digital Watermarking* (Lecture Notes in Computer Science), vol. 5041, Y. Shi, H.-J. Kim, and S. Katzenbeisser, Eds. Berlin, Germany: Springer, 2008, pp. 454–466.

[43] A. Al-Haj, "Combined DWT-DCT digital image watermarking," *J. Comput. Sci.*, vol. 3, no. 9, pp. 740–746, Sep. 2007.

[44] H.-T. Hu and L.-Y. Hsu, "Collective blind image watermarking in DWT-DCT domain with adaptive embedding strength governed by quality metrics," *Multimedia Tools Appl.*, vol. 76, no. 5, pp. 6575–6594, 2016.

[45] A. K. Singh, B. Kumar, M. Dave, and A. Mohan, "Robust and imperceptible dual watermarking for telemedicine applications," *Wireless Pers. Commun.*, vol. 80, no. 4, pp. 1415–1433, Feb. 2015.

[46] C. Tian, R.-H. Wen, W.-P. Zou, and L.-H. Gong, "Robust and blind watermarking algorithm based on DCT and SVD in the contourlet domain," *Multimdia Tools Appl.*, vol. 76, pp. 7515–7541, Dec. 2020.

[47] M. A. Hajjaji, E.-B. Bourennane, A. B. Abdelali, and A. Mtibaa, "Combining Haar wavelet and Karhunen Loeve transforms for medical images watermarking," *BioMed Res. Int.*, vol. 2014, Apr. 2014, Art. no. 313078.
[48] S. Maheshkar, "Region-based hybrid medical image watermarking for secure telemedicine applications," *Multimedia Tools Appl.*, vol. 76, no. 3, pp. 3617–3647, Feb. 2017.
[49] B. Lei, E.-L. Tan, S. Chen, D. Ni, T. Wang, and H. Lei, "Reversible watermarking scheme for medical image based on differential evolution," *Expert Syst. Appl.*, vol. 41, no. 7, pp. 3178–3188, 2014.
[50] X.-C. Yuan and M. Li, "Local multi-watermarking method based on robust and adaptive feature extraction," *Signal Process.*, vol. 149, pp. 103–117, Aug. 2018.
[51] A. K. Singh, B. Kumar, M. Dave, and A. Mohan, "Multiple watermarking on medical images using selective discrete wavelet transform coefficients," *J. Med. Imag. Health Informat.*, vol. 5, no. 3, pp. 607–614, Jun. 2015.
[52] S. A. Parah, J. A. Shaikh, F. Ahaad, N. A. Loan, and G. M. Bhat, "Information hiding in medical images: A robust medical image watermarking system for E-healthcare," *Multimedia Tools Appl.*, vol. 76, pp. 1–35, Dec. 2015.
[53] F. Kahlessenane, A. Khaldi, R. Kafi, and S. Euschi, "A robust blind medical image watermarking approach for telemedicine applications," *Cluster Comput.*, vol. 24, pp. 2069–2082, Feb. 2021.

ALI ALZAHRANI received the B.Eng. degree in computer engineering from Umm Al-Qura University, Makkah, Saudi Arabia, and the M.Sc. and Ph.D. degrees in computer engineering from the University of Victoria, Victoria, BC, Canada, in 2015 and 2018, respectively. He is currently an Assistant Professor with the Department of Computer Engineering, King Faisal University. His research interests include cybersecurity, cryptography, image processing, and systems-on-chip.

NISAR AHMED MEMON received the bachelor's degree in computer systems engineering from Mehran University, Jamshoro, Pakistan, in 1989, and the M.S. and Ph.D. degrees in computer engineering from Ghulam Ishaq Khan Institute (GIKI), Pakistan, in 2005 and 2010, respectively. He currently works as an Assistant Professor with the College of Computer Sciences and Information Technology (CCSIT), King Faisal University, Saudi Arabia. He has published more than 40 research articles in international journals and conferences in the field of image processing, data authentication, medial image watermarking, data security, and bioinformatics. His research interests include digital image processing, digital image watermarking, pattern recognition, data authentication, and cryptography.